



Review

Synthesis and Dissolution of Metal Oxides in Ionic Liquids and Deep Eutectic Solvents

Janine Richter ¹  and Michael Ruck ^{1,2,*} 

¹ Faculty of Chemistry and Food Chemistry, Technische Universität Dresden, 01062 Dresden, Germany; janine.richter4@tu-dresden.de

² Max Planck Institute for Chemical Physics of Solids, Nöthnitzer Strasse 40, 01187 Dresden, Germany

* Correspondence: michael.ruck@tu-dresden.de

Academic Editors: Johan Jacquemin and Fouad Ghamouss

Received: 28 November 2019; Accepted: 19 December 2019; Published: 24 December 2019



Abstract: Ionic liquids (ILs) and deep eutectic solvents (DESs) have proven to be suitable solvents and reactants for low-temperature reactions. To date, several attempts were made to apply this promising class of materials to metal oxide chemistry, which, conventionally, is performed at high temperatures. This review gives an overview about the scientific approaches of the synthesis as well as the dissolution of metal oxides in ILs and DESs. A wide range of metal oxides along with numerous ILs and DESs are covered by this research. With ILs and DESs being involved, many metal oxide phases as well as different particle morphologies were obtained by means of relatively simple reactions paths. By the development of acidic task-specific ILs and DESs, even difficultly soluble metal oxides were dissolved and, hence, made accessible for downstream chemistry. Especially the role of ILs in these reactions is in the focus of discussion.

Keywords: ionic liquid; deep eutectic solvent; metal oxide; dissolution

1. Introduction

Metal oxide materials are of great scientific as well as economic interest because of their versatile utilisation and potential new applications. They are used as functional materials as well as starting substances for the synthesis of diverse task-specific materials. Thereby, their phase, morphology, particle size and purity, often, are of significant importance. Especially for applications, such as catalysis, photovoltaics, and batteries, it is essential to obtain metal oxide particles with specific characteristics, which give control over optical and electronic properties [1]. Thus, for example ZnO, a promising material in the fields of optoelectronics because of its wide band gap (3.3 eV) [2], was synthesised in nano-sized wire [3], rod [4], and tetrapod [5] morphology via template-based sol-gel methods [3], polymer-assisted solution-phase routes [4] and chemical vapour transport [5], respectively. Block-copolymers as a structure-directing template for mesostructured materials have already previously been applied to the synthesis of a large number of metal oxides including Al₂O₃, HfO₂, Nb₂O₅, SnO₂, Ta₂O₅, TiO₂, WO₃ and ZrO₂, as well as the mixed oxides Al₂TiO_x, SiAlO_x, SiTiO_x, ZrTiO_x and ZrW₂O_x [6]. Furthermore, rare earths, such as CeO₂, are of increasing interest for a wide range of applications, e.g., as catalysts, oxygen sensors, and UV absorbers [7]. To synthesise these materials in desired morphologies, hydrothermal [8] and solvothermal [9] methods, microwave-assisted hydrothermal methods [10], thermal decomposition of precursors [11], the sol-gel process [12] and gas condensation [13] have been used. However, these methods often have some drawbacks like high temperatures or pressures, toxic and volatile organic solvents, and expensive starting materials.

Besides their (potential) industrial applications, metal oxides are also important starting materials for the synthesis of metals or diverse metal compounds. Based on naturally occurring ores, earths

and minerals, the production of these chemicals, usually, involves high temperatures. Industrially very important examples are iron, aluminium and titanium [14] which are produced from their oxidic ores at temperatures around 1000 °C [15]. With fossil fuels still dominating the energy market, the large amounts of energy consumed involves high CO₂ emissions. Furthermore, hydrometallurgical methods are applied [16], however, this often is accompanied by the simultaneous dissolution of undesired materials [17]. In addition, metal oxides are present in nuclear waste, where large amounts of secondary waste are generated in the course of metal extraction [18].

In times of climate change and an increasing shortage of non-renewable energy resources as well as waste problems in many parts of the world, the high energy and resource demand for the synthesis as well as the processing of metal oxides has to be reconsidered. Promising alternative solvents for inorganic reactions at low temperatures are ionic liquids (ILs) and deep eutectic solvents (DESs). ILs, by definition, are salts with a melting point below 100 °C. Their favourable properties, such as a negligible vapour pressure, a wide liquid range, good thermal and chemical stability as well as the ability to dissolve a large number of substances, make them an interesting reaction medium for low-temperature synthesis [19]. Similar properties are found for DESs, which are eutectic mixtures of Brønsted or Lewis acids and bases that contain large, asymmetric ionic species. The crucial difference between ILs and DESs is the wide variety of ionic species present in DESs, while ILs mainly consist of one discrete type of anion and cation [20].

The present review article summarises the current state of knowledge on metal oxide chemistry in ILs and DESs in order to provide researchers an overview about the synthetic approaches. Several review articles cover some fields in metal oxide chemistry [21–23], however, no comprehensive summary about the state of knowledge regarding this topic exists. In the following, the first section is concerned with the synthesis of metal oxides, while the second part introduces the dissolution chemistry of metal oxides in ILs and DESs. An overview about the abbreviations used in this article is given in Table 1. The structural formulas of cations and anions of the discussed ILs are presented in Figure 1. The focus is on metal oxide chemistry, therefore, metalloids mostly are neglected.

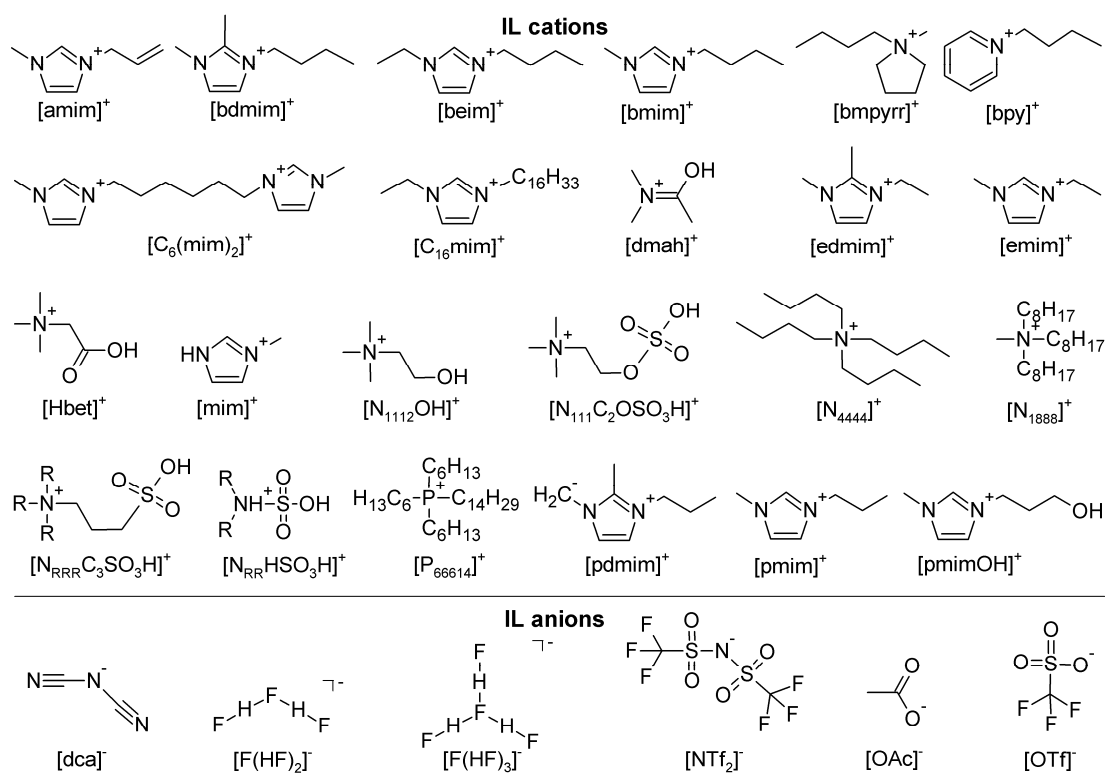


Figure 1. Structures of IL cations and anions addressed in this review.

Table 1. Synopsis of used abbreviations of cations and anions of Ionic liquids (ILs) as well as other reagents in the review.

Abbreviation	Full Name
[amim] ⁺	1-allyl-3-methylimidazolium cation
[bdmim] ⁺	1-butyl-2,3-dimethylimidazolium cation
[beim] ⁺	1-butyl-3-ethylimidazolium cation
bet	betaine
[bmim] ⁺	1-butyl-3-methylimidazolium cation
[bmpyrr] ⁺	1-butyl-1-methylpyrrolidinium cation
[bpy] ⁺	1-butylpyridinium cation
[C ₆ (mim) ₂] ²⁺	6-bis(3-methylimidazolium-1-yl)hexane cation
[C ₁₆ mim] ⁺	1-hexadecyl-3-methylimidazolium cation
[dca] ⁻	dicyanamide anion
[dmah] ⁺	N,N-dimethylacetamidium cation
[edmim] ⁺	1-ethyl-2,3-dimethylimidazolium cation
[emim] ⁺	1-ethyl-3-methylimidazolium cation
[F(HF) _n] ⁻	fluorohydrogenate anion
[Hbet] ⁺	betainium cation
[mim] ⁺	1-methylimidazolium cation
[N ₁₁₂ OH] ⁺	2-hydroxyethyltrimethylammonium cation
[N ₁₁₁ C ₂ OSO ₃ H] ⁺	trimethylammoniummethane hydrogen sulfate cation
[N ₄₄₄₄] ⁺	tetrabutylammonium cation
[N ₁₈₈₈] ⁺	methyltrioctylammonium cation
[N _{RRR} C ₃ SO ₃ H] ⁺	trialkylammoniumpropanesulfonic acid cation
[N _{RR} H ₂ SO ₃ H] ⁺	dialkylsulfamic acid cation
[NTf ₂] ⁻	bis(trifluoromethylsulfonyl)imide anion
[OAc] ⁻	acetate anion
OBu ⁻	butoxide
O ⁱ Pr ⁻	isopropoxide
[OTf] ⁻	trifluoromethanesulfonate anion
[P ₆₆₆₁₄] ⁺	trihexyltetradecylphosphonium cation
[P _{RRR} C ₃ SO ₃ H] ⁺	trialkylphosphoniumpropanesulfonic acid cation
[pdmim] ⁺	1-propyl-2,3-dimethylimidazolium cation
[pmim] ⁺	1-propyl-3-methylimidazolium cation
[pmimOH] ⁺	1-(3-hydroxypropyl)-3-methylimidazolium cation

2. Synthesis of Metal Oxides

2.1. Reactions in ILs

To date, several methods have been published with ILs being used to synthesise metal oxides. However, often ILs merely act as a template to obtain desired phases or morphologies of metal oxides and are not essential for the reaction itself. Especially a better control of nanoparticle synthesis by ILs has been of great scientific interest. Because of the formation of extended hydrogen bond systems in other solvents, many ILs are suitable templates, providing a highly structured reaction environment [24]. Especially in solvothermal synthesis, ILs are added in order to form suitable templates [25]. However, this review is not concerned with the template effect of small amounts of ILs as additives, therefore, in the following, we will not consider reactions in solutions of water or other solvents as major component. Instead, the focus will be on the synthesis of metal oxides in ILs acting as solvent or even reaction partner.

Three main synthesis methods in ILs are popular, which are ionothermal, microwave-assisted and sonochemical reactions. Based on the hydrothermal reactions, ionothermal means the heating of a reaction mixture in an IL instead of water as a reaction medium. Because of the low vapour pressure of ILs, no high autogenous pressure builds up, which is why ionothermal reactions often take place at or close to ambient pressure [26]. ILs are particularly suitable for microwave heating. Because of their large, highly polarisable cations, a very efficient absorption of microwave irradiation makes them an effective heating medium for microwave-assisted synthesis [27]. Recently, also the combination of sonochemistry and ILs has been reported [28–31]. Based on the phenomenon of acoustic cavitation,

ultrasound irradiation produces so-called cavitation bubbles which generate very high temperatures and pressures when collapsing [32,33]. All three methods are applied to metal oxide synthesis in ILs.

2.1.1. Titanium Oxide

Among the metal oxides synthesised in ILs, TiO_2 plays a major role, as already highlighted in a review by Voepel and Smarsly [34]. TiO_2 exists in several phases, the most common ones being rutile, anatase and brookite. In aqueous medium, rutile is the most stable phase for macroscopic particles. However, decreasing the size to nanoparticles, anatase is favoured [35].

The general procedure for the IL-assisted synthesis of TiO_2 is the dissolution of either TiCl_4 or $\text{Ti}(\text{O}^i\text{Pr})_4$ in a mixture of an IL and water and subsequent heating. It is apparent from the fact that water alone hydrolyses these titanium salts very readily to TiO_2 [36], that ILs in these systems merely act as templates. Nevertheless, a wide variety of morphologies as well as improved phase control is accessible by IL-assisted syntheses.

Using ionothermal heating of TiCl_4 (100 °C, 14 h), Smarsly et al. found, that the phase of titania nanoparticles is controllable by the IL's anion. Apparently, the $[\text{NTf}_2]^-$ anions of the ILs $[\text{emim}][\text{NTf}_2]$, $[\text{bmpyrr}][\text{NTf}_2]$ and $[\text{P}_{66614}][\text{NTf}_2]$ stabilise an amorphous TiO_2 phase which spontaneously crystallises into rutile during IL extraction with isopropyl alcohol. The $[\text{NTf}_2]^-$ anion could either be an acceptor for the protons forming during the reaction, subsequently, acting as a surfactant, or directly interact with the titania species. Comparing the (110) surface of rutile and anatase, a significantly higher amount of unsaturated titanium atoms is found for the former, which readily react with the electron lone pair of $[\text{NTf}_2]^-$. Thus, assumedly, in the presence of $[\text{NTf}_2]^-$, an intermediate amorphous titanium oxide phase is formed, which favours the subsequent crystallisation into rutile. For this reaction to take place, also the amount of water has to be kept low, in order to avoid the formation of anatase particles usually taking place in aqueous medium. In contrast to that, reactions in $[\text{bmim}][\text{BF}_4]$, $[\text{C}_{16}\text{mim}]\text{Cl}$ and $[\text{emim}][\text{BF}_4]$ yield anatase [37].

The same result was found by Zhou and Antonietti, using TiCl_4 and the IL $[\text{bmim}][\text{BF}_4]$ as the starting materials and an ionothermal approach (80 °C, 12 h) to obtain anatase nanoparticles that assemble to mesoporous spherical particles. The IL, apparently, favours a reaction-limited aggregation mechanism, resulting in very small primary particles with a size of only 2–3 nm [38].

Using the same IL, Liu et al. synthesised phase-pure anatase nanoparticles from $\text{Ti}(\text{O}^i\text{Pr})_4$ in a microwave-assisted heating method (126 W, 40 min). According to them, the hydrolysis of $\text{Ti}(\text{O}^i\text{Pr})_4$ leads to the condensation into short-chain polyanions, which are protected as dissolved intermediates by $[\text{bmim}]^+$. Only with a fast temperature increase, rapid crystal growth occurred. In this process, the $[\text{bmim}]^+$ cation, apparently, protects the seed crystals, as less preferred crystal growth was observed, yielding truncated bipyramid particles [39].

Furthermore, anatase was synthesised by Mudring et al. in a sonochemical reaction (45 kHz, 60 W, 9 h) by dissolving $\text{Ti}(\text{O}^i\text{Pr})_4$ in the IL $[\text{pmimOH}][\text{NTf}_2]$. With a particle size of 5 nm, anatase is the most stable product phase to be expected, however, the synthesis at ambient conditions poses some difficulties, that can be overcome by this IL-assisted, sonochemical method. Furthermore, the IL as a template supports the formation of spherical particles [31]. The $[\text{pmimOH}]^+$ cation owns not only an acidic proton at the imidazolium core, but also a hydroxyl group, that could offer strong interactions [40].

Additionally, the group presented a systematic study about the synthesis of TiO_2 in ILs and the influence of the reaction parameters, such as the titanium precursor, the cation of the IL, the heating method and the pH value. The different ILs were chosen in order to provide different ways of potential interaction: via π - π -interactions of an aromatic core ($[\text{bpy}][\text{NTf}_2]$), an aromatic system and an acidic proton ($[\text{bmim}][\text{NTf}_2]$), none of both ($[\text{N}_{1888}][\text{NTf}_2]$, $[\text{P}_{66614}][\text{NTf}_2]$) or an additional functional group ($[\text{pmimOH}][\text{NTf}_2]$). Apparently, by sonochemical heating (45 kHz, 60 °C, RT, 9 h) of $\text{Ti}(\text{O}^i\text{Pr})_4$ in every IL, different product morphologies were obtained, highlighting the different interactions between the IL cation the product particles. Furthermore, only $[\text{pmimOH}]$ supports the formation of phase

pure anatase, while in all other ILs, mixtures of brookite and anatase are formed. The use of TiCl_4 as starting material, instead, favours the formation of rutile. This is attributed to the formation of HCl during hydrolysis. In agreement with this, pH investigations yielded rutile by the addition of HCl, but anatase when adding urea. Interestingly, this is contrary to the previously mentioned reports [37,38], where anatase was obtained despite using a chloride IL or TiCl_4 as the starting material. Investigating the heating method, sonochemical and ionothermal (170 °C, 2 h) heating gave anatase particles varying morphologies, however, a microwave-heated (2.45 GHz, 80 °C, 10 min) sample contained significant amounts of brookite alongside [40]. This extensive study shows that the control of phase and morphology of metal oxides in ILs depends on various factors. General statements are difficult to make as the underlying mechanisms for the effects of reaction partners and conditions are not understood, yet. It might be an interesting observation, that [pmimOH][NTf₂], strongly interacting because of its functional group, shows the most structure-directing effect, yielding no side phases. In contrast to the report by Smarsly et al. [37], the [NTf₂][−] anions of the ILs used did not support the crystallisation in rutile phase. Apparently, the higher reaction temperature or other heating methods suppress the structure-directing effect of this anion.

A different approach, without heating even being necessary, was reported by Nakashima and Kimizuka who used an interfacial sol-gel process to synthesise hollow TiO_2 microspheres. For this purpose, they added a solution of $\text{Ti}(\text{O}i\text{Bu})_4$ in toluene to the IL [bmim][PF₆] under constant stirring. As toluene is poorly soluble in the IL, a microemulsion formed with $\text{Ti}(\text{O}i\text{Bu})_4$ being hydrolysed by water traces at the toluene droplet-[bmim][PF₆] interface. The obtained gel consists of amorphous TiO_2 and can be transformed into anatase by calcination (500 °C, 5 h). According to the authors, this method can also be applied to $\text{Hf}(\text{O}i\text{Bu})_4$, $\text{InSn}_3(\text{OR})_x$, $\text{Nb}(\text{O}i\text{Bu})_5$ and $\text{Zr}(\text{O}i\text{Bu})_4$ [41].

Another interesting field in TiO_2 chemistry is the synthesis of the metastable bronze phase $\text{TiO}_2(\text{B})$ because of its lithium ion storage capacity [42–44] and potential photocatalytic applications [45,46]. Several research groups have synthesised this compound with a similar ionothermal method by adding TiCl_4 and a small amount of water for hydrolysis to a mixture of [bmim]Cl, [bmim][BF₄], [C₁₆mim]Cl and [C₁₆mim][BF₄] at 95 °C [46–50]. Smarsly et al. identified the partly hydrolysis of the [BF₄][−] anion and the subsequent provision of fluoride ions as crucial for the formation of $\text{TiO}_2(\text{B})$. According to them, fluoride through coordination with titanium inhibits the formation of titanium oxyhydroxy clusters supporting the formation of the layered $\text{TiO}_2(\text{B})$ structure. Depending in the ratio of the four ILs, a different product composition ranging from phase pure $\text{TiO}_2(\text{B})$ to anatase, rutile or titanium hydroxyoxyfluoride as additional phases, is found [48]. This research highlights additional difficulties for the prediction of reaction outcomes when working in mixtures of different ILs as they might show a non-linear behaviour upon mixing in varying compositions. Due to the complexity of this system, further investigations need to reveal the reaction mechanisms present.

2.1.2. Zinc Oxide

Mesocrystals of ZnO were synthesised in the highly hydrated IL [N₄₄₄₄]OH (often abbreviated as TBAH), as shown by Taubert et al. Refluxing a solution of $\text{Zn}(\text{CH}_3\text{COO})_2$ in [N₄₄₄₄]OH (100 °C, 20 h) yielded nano-sized ZnO particles. For low $\text{Zn}(\text{CH}_3\text{COO})_2$ concentrations, these primary particles assembled to hollow spheres on the glass wall of the reaction vessel. A large effect on the product morphology is ascribed to the intrinsic electric fields of the polar ZnO lattice. Thereby, the [N₄₄₄₄]⁺ cation might reverse the polarity of the individual particles, thus, preventing further growth and supporting the aggregation to a mesostructure [51]. The product morphology strongly depends on the reaction temperature, as after three days at room temperature, the rod-like primary particles assembled to solid mesocrystals. [52]. Previously, the group had shown that ZnO can also emerge from polymer-controlled reactions of aqueous $\text{Zn}(\text{NO}_3)_2$ solutions that are heated to 90 °C [53–55], but mesocrystals like the ones observed require the presence of [N₄₄₄₄]OH [52].

A sonochemical synthesis (45 kHz, 60 W, RT, 12/24 h) for ZnO was found by Mudring et al. Starting from the acetate salt, phase-pure wurtzite nanorods were obtained in the IL [bmim][NTf₂] in

the presence of NaOH [28]. Presumably, the IL in this case merely acts as a solvent and the reaction forming the metal oxide might be ascribed to the high temperatures occurring because of the ultrasound irradiation and leading to the decomposition of the acetates. In experiments, temperatures of several thousand Kelvin in the cavitation bubbles were found [32], while for $\text{Zn}(\text{CH}_3\text{COO})_2$ a complete decomposition to ZnO was reported at 530 °C [56].

ZnO was also synthesised by Zheng et al. in the ILs [emim][BF₄], [bmim][BF₄] and [bdmim][BF₄] from $\text{Zn}(\text{CH}_3\text{COO})_2 \cdot 2\text{H}_2\text{O}$ (80 °C, 48 h) [57]. With the underlying synthesis method, a low-temperature solid state reaction, nanocrystals of metal oxides can be produced from hydrated metal salts in the presence on NaOH [58]. However, the presence of ILs provides suitable templates for the synthesis of tailored 1D nanostructures. On one side, the presence of a proton at the C2 position of the imidazolium cation is crucial for the ability to form hydrogen bonds to the oxygen atoms of ZnO, thus, influencing the growing direction of the particle. On the other side, also the length of the alkyl chain on the imidazolium ring can affect the particle size because of steric hindrance [57].

In another attempt to synthesise ZnO, Dai et al. investigated ILs not only acting as a solvent but as a precursor for the product. The synthesised tailored ILs consist of complex zinc-alkylamine cations and [NTf₂][−] anions. Together with a small amount of tetramethylammonium hydroxide, enabling nucleation formation through hydrolysis, the IL yields ZnO under ionothermal conditions (110 °C, several hours). The products are micrometer-sized particles consisting of nanostructures. The morphology strongly depends on various factors, including ligand size and temperature as the most affecting [59]. Using such approaches with the metal cation being part of the IL, the synthetic effort has to be considered as well as the fact that the reaction takes place under consumption of the IL. Regarding the previously mentioned studies, more efficient synthesis methods are assumed to be developable.

2.1.3. Copper Oxide

Two synthetically easy, low temperature-approaches similar to the methods for ZnO formation were applied to CuO as well. Hence, CuO can be synthesised in the IL [N₄₄₄₄][OH] ionothermally from $\text{Cu}(\text{CH}_3\text{COO})_2$. Mechanistic studies revealed the completion of the reaction to CuO already after one minute at 40 °C and even faster at higher temperatures. The formation of the product takes place in a two-step reaction with intermediate $\text{Cu}(\text{OH})_2$ rods which subsequently aggregate and dehydrate to single-crystalline CuO nanoplates. However, a subsequent heat treatment at 250 °C to 300 °C is necessary in order to remove adherent traces of the IL [60].

Mudring et al. also synthesised CuO sonochemically from $\text{Cu}(\text{CH}_3\text{COO})_2$ in the presence of NaOH (45 kHz, 60 W, RT, 12/24 h). While the decomposition of the acetate (decomposition temperature 355 °C [56]) assumedly can be ascribed to effect of acoustic cavitation, the IL might act as a template for a nanorod morphology. This reaction yielding relatively uniform particles with an enlarged band gap compared to the bulk material, might be promising for potential applications [29].

2.1.4. Iron Oxides

For the iron oxides Fe₂O₃ and Fe₃O₄, different IL-assisted synthesis methods were found. Similar to ZnO and CuO, γ -Fe₂O₃ as well as Fe₃O₄ were synthesised in the highly hydrated IL [N₄₄₄₄][OH] from $\text{Fe}(\text{CH}_3\text{COO})_2$ (100 °C, 10 h). The products were mostly obtained in cubic morphology, although spherical particles were present. According to the authors, this method is quite simple compared to other approaches yielding iron oxide particles of a similar size (8 nm in diameter) [61]. However, as both iron oxides are obtained simultaneously, synthesis optimisation is necessary for practically relevant phase-pure products.

A phase-pure synthesis of α -Fe₂O₃ in an ionothermal reaction (180 °C, 12 h) from $\text{FeCl}_3 \cdot 12\text{H}_2\text{O}$ in [pmim]I was reported by Zheng et al. [62]. This reaction also readily takes place in water [15], however, the product was obtained as nanoplatelets assembled to nanoplates. Presumably, the IL neutralises ionic charges at the surface of the nucleus in *c*-direction, thus preventing crystal growth along this

plane. The aggregation of the resulting nanoplatelets to regular nanoplates is ascribed to the ability of the IL to form two-dimensional polymeric assemblies. Studies in a mixed solvent of [pmim]I and water showed that the latter disturbs this mechanism, yielding randomly assembled nanoplatelets [62].

Furthermore, Yang et al. reported the ionothermal synthesis of γ -Fe₂O₃ from Fe(CO)₅ in the IL [bmim][NTf₂] (280 °C, 1 h). The reaction, apparently, takes place by the decomposition of Fe(CO)₅ and the subsequent oxidation to iron(III) by oxygen in the air or its traces in argon atmosphere. Oleic acid added besides acts as a capping agent supporting the formation of nanoparticles with a quite narrow particle size distribution. Nanoparticles of the same quality can also be received by reusing the IL, thus, presenting an applicable way of recycling [63].

A microwave-assisted method (2.45 GHz, 900 W) for the synthesis of Fe₂O₃ was reported by Gedanken et al. who showed that Fe(NO₃)₃ reacts to Fe₂O₃ nanoparticles with air oxygen in the IL [bmim][BF₄]. This is only observed for a short heating period of 2 minutes. After longer irradiation time, the decomposition of the IL takes place involving the reduction of iron(III) to iron(II) by carbon and the formation of FeF₂ using fluoride from the IL's hydrolysed [BF₄][−] anion [64].

2.1.5. Cerium Oxide

Similar to the systematic study on TiO₂ synthesis in ILs, Mudring et al. investigated the formation of CeO₂, particularly the influence of the cerium precursor, the cation of the IL, the heating method and the precipitator (NaOH, NH₄OH). Like in the TiO₂ synthesis, the ILs act as a template while the hydrolysis of the cerium precursors can be ascribed to NaOH or NH₄OH, respectively [36]. Only ultrasound irradiation (45 kHz, 60 W, RT, 12 h) yielded phase-pure CeO₂, whereas microwave (2.45 GHz, 80 °C, 10 min) and ionothermal (170 °C, 20 h) heating also produced Ce₂O₃ and Ce(OH)₃ by-products, which can be converted into CeO₂ via calcination (425 °C, 4 h) [30]. This might be ascribed to the higher temperatures already present in the cavitation bubbles during sonochemical heating. For the sonochemical reaction pathway, an increase in crystallinity of the aggregated nanospheres with increased irradiation time is observed. Using different cerium precursors (Ce(CH₃COO)₃, Ce(NO₃)₃, CeCl₃) and ILs has no influence on the phase purity of the CeO₂ obtained, but, as well as the precipitant, influences the morphology of the nano-sized products. This is ascribed to varying reaction kinetics. Hence, different precursors possess varying hydrolysis rates and, furthermore, the counter ion can influence the morphology by favoured coordination to certain crystal facets. Different IL cations were chosen because of their different potential interactions including a π -system ([bpy][NTf₂], [edimim][NTf₂]), an additional acidic proton ([bmim][NTf₂]), none of both ([bmpyrr][NTf₂]) or a functional group ([N₁₁₁₂OH][NTf₂]). These different interactions result in different product morphologies with the mechanisms not being clear, yet [30]. This study again shows the huge influence of a wide variety of reaction parameters on the obtained product.

Using a similar ionothermal approach (150 °C, 2 h), Yu et al. synthesised CeO₂ nanoparticles in [emim][NTf₂] with NaOH as precipitator. However, apparently the interactions between the IL and the ceria nanoparticles are relatively high, making calcination (600 °C, 2 h) necessary for the removal of the IL. According to the authors, the resulting CeO₂ is phase-pure with no evidence for impurities [65].

Furthermore, Yan et al. synthesised CeO₂ from Ce(NO₃)₃·6H₂O in the IL [C₁₆mim]Br (100 °C, 2d). Despite ethanol being used for a better dissolution of the starting material, apparently, no additional precipitator is necessary to obtain the oxide. The IL played the role of a solvent as well as a template for nearly monodisperse spherical ceria nanoparticles. The template effect is assumed to be mediated via hydrogen bonding between the IL and cerium hydroxide and π - π -stacking of the imidazolium rings [66].

Mixed oxides of cerium, namely the CO oxidation catalysts Ce_{0.5}M_{0.5}O₂ (M = Ti, Zr, Hf), were synthesised by Mudring et al. in the IL [bmim][NTf₂] by ionothermal (170 °C, 20 h), microwave (2.45 GHz, 80 °C, 10 min) and sonochemical (45 kHz, 60 W, RT, 9 h) methods. The best catalytic activity of the directly obtained, highly crystalline materials was found for the microwave-heated products. An exchange of the IL's cation by [P₆₆₆₁₄]⁺ yielded similar spherical nanoparticles. However,

using $[\text{pmimOH}]^+$, which offers significantly stronger interactions via hydrogen bonding, resulted in sheet-like nanoparticle assemblies for $\text{Ce}_{0.5}\text{Zr}_{0.5}\text{O}_2$ [67].

2.1.6. Miscellaneous

For several metal oxides, relatively isolated reports concerning their synthesis in ILs are found. A promising ionothermal method to synthesise $\gamma\text{-Al}_2\text{O}_3$ from an IL without the usually necessary annealing step was reported by Zheng et al. Through heating (150 °C, 10 h) of AlCl_3 in $[\text{bdmim}]\text{Cl}$ in the presence of sodium amide (NaNH_2), crystalline nanoparticles of $\gamma\text{-Al}_2\text{O}_3$ aggregating to mesoporous nanoflakes were obtained. The IL, in this case, acts as a solvent as well as a template for the worm-like pores. A mechanism is proposed with AlCl_3 initially reacting to $\text{Al}(\text{OH})_3$ with NaNH_2 and traces of water in the IL. Subsequently, Al_2O_3 forms under ionothermal conditions. Apparently, in this reaction, Al_2O_3 is synthesised at the lowest temperature reported so far [68]. Despite a few research groups describing synthesis routes of Al_2O_3 in ILs [69–72], the one reported by Zheng et al. appears to be the only one yielding alumina without calcination. Therefore, it would be especially interesting to figure out the processes taking place in the IL in future research.

PbO was obtained in a PbS-type crystal structure by Li Juan et al. starting from $\text{Pb}(\text{OH})_2$ by an ionothermal reaction (180 °C, 3 h) in the IL $[\text{beim}][\text{BF}_4]$. The reaction taking place, merely is the thermal decomposition of $\text{Pb}(\text{OH})_2$ (decomposition temperature 145 °C [36]), however, the IL acts as template for the crystal structure. So far, no mechanism is suggested for the role of the IL [73].

Tin doped In_2O_3 was synthesised in a microwave-assisted approach from SnCl_4 and $\text{InCl}_3 \cdot 4\text{H}_2\text{O}$ in the IL $[\text{N}_{1444}][\text{NTf}_2]$ in the presence of DMF and $[\text{N}_{1111}]\text{OH}$ by Feldmann et al. (300 °C, 15 s). The nanocrystalline product was obtained in thin, transparent layers allowing the utilisation as electrode material. Thereby, the IL appears to be crucial for charge stabilisation, thus, avoiding particle agglomeration [74].

The same IL was used for the synthesis of the manganese oxides hydrohausmannite and Mn_3O_4 in the shape of nanodisks by Taubert et al. (100 °C, 10 h). However, this mixture of manganese oxides had to be calcined in order to yield phase-pure Mn_3O_4 . Despite a small amount of water was added in order to improve the solubility of $\text{Mn}(\text{CH}_3\text{COO})_2$, the authors claim that this can be avoided by the use of other manganese salts than $\text{Mn}(\text{CH}_3\text{COO})_2$ [61].

$[\text{N}_{4444}]\text{OH}$ was also applied to the ionothermal synthesis of the phase-pure mixed metal oxide SrTiO_3 by Ruck et al. (180 °C, 20 h). Apparently, at the beginning of the reaction, $\text{Ti}(\text{O}^i\text{Pr})_4$ is hydrolysed to form an amorphous intermediate, which subsequently reacts with strontium(II) cations. Thereby, the morphology of the intermediate is preserved. A specific amount of IL is necessary to achieve the completeness of the reaction, however, in its hydroxide ion providing function, it can be replaced by other bases, e.g., NaOH . Altogether, in this synthesis, particle sizes in the range of 50–150 nm were obtained, whereby the desert-rose-like morphology depends on the presence of ethylene glycol [75].

2.1.7. Conclusion on IL-Based Metal Oxide Synthesis

In so far investigated systems, ILs most commonly act as solvent and template in ionothermal, microwave-assisted and sonochemical reactions that take place in IL-free solvents as well. However, a better control of phase and morphology of the often nanostructured metal oxides is possible. This is due to the interactions between the IL and the metal oxidic nuclei. In most cases, the role of the cation is considered more important as hydrogen bonds as well as $\pi\text{-}\pi$ -interactions can be formed. However, the effect of the anions, despite just weakly coordinating, should not be neglected.

Understanding some effects of ILs should not hide the fact, that their role and reaction mechanisms, in many cases, are not clarified at all. Previous investigations have been of rather empirical nature, whereas further studies could support models for the prediction of reactions. It should also be taken into account, that the reaction outcome not only depends on the IL, but various factors, such as heating method, reaction temperature and additives, have a significant effect on the product, which is not

completely understood, yet. Also, effects of the concentration of the IL, respectively the amount of additives, and the composition of IL mixtures should be investigated in more detail.

The previously discussed synthetic approaches, in many cases, stand out because of their relative experimental straightforwardness. Therefore, the application of ILs could mean a significant simplification for the synthesis of defined metal oxide phases compared to conventional methods. However, it has to be taken into account, that for most applications a separation of the metal oxide particles from the IL is necessary. This can be performed by relatively uncomplicated washing with suitable solvents or in some cases, calcination might be needed. As for nanoparticles, already small traces of adherent IL might change their properties, their purity should always be questioned critically and examined by suitable methods, such as IR, Raman or energy-dispersive X-ray spectroscopy.

Thus, ILs are a promising reaction medium for the synthesis of metal oxide particles in well-defined shapes, but a comprehensive understanding still lacks systematic data.

Furthermore, a promising approach for a completely new reaction pathway for metal oxide synthesis is reported by Zheng et al. who synthesised γ - Al_2O_3 at only 150 °C, a significant decrease compared to conventional calcination. Systematic studies could give valuable information about a more efficient synthesis of Al_2O_3 and other metal oxides. Especially the mechanism of this ionothermal synthesis is of great interest.

2.2. Reactions in DESs

A reaction medium with very similar characteristics and properties to ILs are DESs. Most common DESs are mixtures formed by a quaternary ammonium salt and a hydrogen bond donor [20,76,77]. Characteristic for DESs is the low melting point, which is significantly below the melting points of the individual components. This is illustrated by the example of the very popular nontoxic and cheap choline chloride-urea DES (molar ratio 1:2). While choline chloride and urea melt at 302 °C and 133 °C, respectively, the DES has a melting point of only 12 °C, which is ascribed to the strong hydrogen bonds in the solution [20]. Most approaches for metal oxide synthesis described below were performed in this DES, choline chloride-urea (molar ratio 1:2), taking advantage of the decomposition of urea at temperatures above 100 °C, which produces NH_3 . Apparently, these NH_3 molecules form intermediate ammine complexes and, thus, play an important role as a template for nanostructures or as a reactant [78–82].

2.2.1. Zinc Oxide

In a DES formed from oleic acid and different alkyl amines, Xie et al. synthesised ZnO micro-pyramids from zinc acetate (286 °C, 1 h). The thermal decomposition of the reagent takes place in non-DES solvents as well forming wurtzite ZnO of irregular or nanorod morphology. However, the DES, apparently, lowers the surface energy of the polar surfaces, hence, supporting the growth of hexagonal micro-pyramids [83].

2.2.2. Iron Oxides

Tu et al. synthesised α - Fe_2O_3 from FeCl_3 in a reaction at 200 °C in choline chloride-urea (molar ratio 1:2). NH_3 arising from decomposed urea plays an important role in the proposed mechanism to form the complex intermediate $\text{Fe}(\text{NH}_3)_2\text{Cl}_3$ that reacts with Fe_2O_3 after the addition of water. Thereby, Fe_2O_3 in the form of nanospindles is obtained [84].

A microwave-assisted reaction to Fe_2O_3 was applied by Edler et al. heating $\text{Fe}(\text{NO}_3)_3 \cdot 9\text{H}_2\text{O}$ in choline chloride-urea (molar ratio 1:2, 300 W, 100–200 °C, 10 min). Phase, size and morphology of the obtained particles depend on the reaction temperature and the water content. This is attributed to the decomposition of urea depending on both factors. Hence, γ - Fe_2O_3 was obtained at 150 °C, but α - Fe_2O_3 at 200 °C. Altogether, the addition of small amounts of water was found to have a positive effect, due to a lower viscosity and the supported hydrolysis of urea. [85].

Another iron oxide, Fe_3O_4 , was synthesised by Chen et al. via co-precipitation in choline chloride-urea (molar ratio 1:2). By the heating of FeCl_3 and FeCl_2 ($80\text{ }^\circ\text{C}$, 1.5 h), spherical, magnetic Fe_3O_4 nanoparticles were obtained. As the product particles are more regular and smaller than the products obtained when the same reaction is carried out in water, the DES apparently acts as a template during the nanoparticle formation. Despite no hydrolysis of urea taking place at the reaction temperature, mostly the choline cations are assumed to be absorbed at the Fe_3O_4 particle surface, preventing uncontrolled growth [78]. A method without the decomposition of urea has the advantage of being potentially recyclable, hence, more efficient.

2.2.3. Tin Oxides

Gu et al. synthesised SnO from SnCl_2 in choline chloride-urea (molar ratio 1:2, $100\text{ }^\circ\text{C}$, 1–60 min). A reaction mechanism is proposed with SnCl_2 , at first, reacting to $\text{Sn}(\text{OH})\text{Cl}$ with traces of water in the DES. Subsequently, the reaction with ammonia released from urea yields SnO and NH_4Cl . The SnO particles obtained are nano- and microsized because of the fine dispersion in the solution. Apparently, oxygen in the air causes the oxidation to SnO_2 [86].

Furthermore, they found a method to synthesise SnO_2 /graphene nanocomposites from SnCl_2 and graphene oxide sheets in an ultrasound-assisted reaction in choline chloride-urea (molar ratio 1:2, RT, 4 h). A mechanism is suggested with graphene oxide being reduced by SnCl_2 and subsequent SnO_2 deposition on the graphene sheets. The advantage of this DES reaction medium, according to the authors, is the uncomplicated experimental setup [80]. However, such SnO_2 /graphene composites can also be synthesised in other reaction mediums, like a water-HCl-urea mixture [87].

The group also used $\text{N}_2\text{H}_4\cdot\text{H}_2\text{O}$ as additive for the synthesis of nanograined SnO_2 from $\text{SnCl}_2\cdot 2\text{H}_2\text{O}$ in the DES choline chloride-urea (molar ratio 1:2, 1 h). A mechanism is proposed with $\text{N}_2\text{H}_4\cdot\text{H}_2\text{O}$ reducing tin(II) to tin(0) nanoparticles. The DES, subsequently, prevents the agglomeration of the particles, which allows the reaction with oxygen because of their high reactivity [88].

2.2.4. Miscellaneous

Another DES applied to metal oxide synthesis is choline chloride-ethylene glycol (molar ratio 1:2). With the additional help of acetic acid, Fu et al. synthesised nanosized cuboctahedral particles of tungsten molybdenum oxide composites from $(\text{NH}_4)_2\text{WO}_4$ and $(\text{NH}_4)_6\text{Mo}_7\text{O}_{24}$ ($40\text{ }^\circ\text{C}$, 6 h). Although no detailed reaction mechanism was proposed, the DES could compensate high surface energies [89].

2.2.5. Conclusion on DES-Based Metal Oxide Synthesis

Only a few experiments regarding the synthesis of metal oxides in DESs have been performed, yet. This research focused on the utilisation of DESs as template for more homogeneous nanostructures of oxide materials that could be obtained in DES-free aqueous solutions as well. From the small amount of data on the synthesis of metal oxides in DESs no predictions of reaction results and promising approaches are possible.

Often the formation of NH_3 from decomposing urea is made use of, which subsequently can act as a reactant. Naturally, the consumption of the DES for a reaction restricts its recyclability. However, because of the lower cost and toxicity of DESs compared with ILs, they might still be valuable reactions systems. Furthermore, a reaction at just $80\text{ }^\circ\text{C}$ without the decomposition of urea showed, that the intact components of DESs can be beneficial for reactions, as well. Therefore, this might be a promising approach for future research.

Despite the small amount of previous research, DESs exhibit favourable dissolution properties, which widely differ from molecular solvents [77]. They could more systematically be applied to different kinds of starting materials in order to find new reaction pathways for the synthesis of metal oxides. Especially their lower cost and higher environmental compatibility compared to many ILs could make them an interesting alternative.

2.3. Hydroxide Synthesis and Calcination

Another approach for the synthesis of metal oxides in ILs or DES is their utilisation for an efficient synthesis of the respective metal hydroxide in a desired morphology followed by an annealing step. This synthesis principle is not uncommon [69–72,90], but as the IL, respectively the DES, only takes part in the formation of a precursor and the energy-consuming calcination step still has to be performed, only a few examples are mentioned here.

Mudring et al. used a microwave-assisted reaction method (2.45 GHz, 80 °C, 10 min) to synthesise SrSnO₃ from Sr(CH₃COO)₂ and SnCl₄ with different ILs ([bmim][NTf₂], [C₆(mim)₂][NTf₂]₂, [bpy][NTf₂], [P₆₆₆₁₄][NTf₂]) in the presence of NaOH acting as solvent and template. The obtained SrSn(OH)₆, subsequently, was calcined (700 °C, 3 h) to yield SrSnO₃ [91]. The reaction was also successfully performed in an ionothermal synthesis (170 °C, 20 h) before calcination [27]. Despite the reaction takes place in aqueous solution, as well, the IL prevents agglomeration and different cations influence the morphology of the nano-SrSnO₃. Thereby, different possible interactions ways, such as hydrogen bonding and π - π -interactions, have significant effects, however, the mechanisms are not understood, yet [91].

The same reaction method has been applied to Sr_{1-x}Ba_xSnO₃ (x = 0; 0.2; 0.4; 0.6; 0.8; 1) using Ba(CH₃COO)₂ as an additional reactant in the IL [bmim][NTf₂]. Solid solutions of SrSnO₃ and BaSnO₃ without any detectable impurities were obtained [27].

Using a DES, Gu et al. synthesised NiO from NiCl₂ in choline chloride-urea (molar ratio 1:2) at 150 °C (40 min). After the addition of water and workup, the Ni(OH)₂ precipitation was annealed (300 °C, 4 h). Nano-sized, flower-shaped NiO built from smaller grains with a mesoporous structure was obtained. The effect, which is used in the DES-reaction, is the decomposition of urea, producing NH₃ that reacts with the well-dispersed water and thereby provides OH⁻ as reaction sites. The experiment was also performed in an aqueous NaOH solution with both reactions yielding phase-pure NiO. As NaOH in the aqueous solution is not as well dispersed, nucleation is far more inhomogeneous [79,81]. Using the same reaction method with slight changes in reaction temperature and time, the research group also obtained Co₃O₄ as mesoporous nanosheets [82].

Furthermore, Su, Wen et al. produced sheets of Na₂Ti₃O₇, interesting as an anode material for sodium-ion batteries in the DES choline chloride-ethylene glycol (molar ratio 1:2, 80 °C). Despite calcination of the precursor (500 °C, 7 h) being necessary, the reaction temperature could significantly be reduced compared to conventional synthesis [92].

Similarly, a γ -CoV₂O₆ precursor was synthesised by Seo et al. in the DES choline chloride-malonic acid (molar ratio 1:1, 100 °C, 2 h). The cobalt vanadate was obtained after additional 2 h calcination at 500 °C, which is significantly lower than the conventional solid-state synthesis at 900 °C in 6 h. The authors suggest that the decomposition of the DES generates in situ high thermal conditions at relatively low temperatures leading to the formation of γ -CoV₂O₆. Furthermore, the DES, apparently, acts as a template for octahedral nanoparticles [93].

The same IL was used by Boston et al. for the synthesis of a barium titanate precursor from barium acetate and titanium isopropoxide. However, the final oxide was obtained after 6-h calcination at 500 °C and 1 h at 950 °C [94].

In a similar approach, Zhang et al. used the DES glucose-urea (molar ratio 1:3) as a reaction medium and template for the catalytically active binary oxide Ir₂SnO_x from the chloride salts (180 °C, 12 h). The elevated temperature causes the polymerisation of glucose, hence, the formation of a foam in which the metal ions are embedded. Carbon is finally removed by calcination at 500 °C yielding porous Ir₂SnO_x in nanorod morphology. According to the authors, urea also plays a crucial role by providing coordinating NH₂ groups which support a uniform composition of the product [95]. At the temperatures used this could rather be NH₃ ligands.

König et al. synthesised spinel-type ferrite nanoparticles MFe₂O₄ (M = Mg, Zn, Co, Ni) by dissolving equimolar amounts of Fe₂O₃ (haematite) and MO (M = Mg, Co, Ni, Zn) in ten different DESs. They consisted of choline chloride, urea or *N,N'*-dimethylurea as hydrogen bond acceptors and

organic acids (maleic, malic, citric acid), sugars (D-mannose, D-fructose, D-glucose), *N,N'*-dimethylurea or vanillin as hydrogen bond donors. In the first step, the dissolution was performed in two hours at 80 °C, subsequently, the ferrite nanoparticles were obtained via calcination at 400–600 °C. Despite calcination being necessary to obtain the product, the reaction temperature was lowered compared to conventional solid state reactions at 900 °C [96]. No reaction mechanism was suggested, however, all DES components contain O and N atoms suitable to coordinate to metal ions, thus supporting the dissolution of the starting materials.

Even if ILs and DES, in several systems, do not give metal oxides as a product, but only the hydroxide precursor, such methods can be beneficial compared to IL- or DES-free approaches. Thus, in many cases the calcination temperature can be lowered, which at least is an auspicious beginning for reducing the amount of energy needed. Furthermore, the interactions of the solvent influence the morphology of the metal hydroxide, which, usually, is preserved in the calcined metal oxide, as well. Thus, ILs and DESs, in these systems, also exhibit a template effect. As many pure metal oxides could be obtained in different phases and morphologies directly in ILs and DESs, the hydroxide calcination approach seems to be rather promising for mixed metal oxides, where less research has been performed, yet.

3. Dissolution of Metal Oxides

3.1. Dissolution in ILs

The processing of metal oxides, present in naturally occurring ores, earths and minerals as well as in (nuclear) waste, with conventional energy- and resource-demanding methods is considered increasingly problematic. In order to find solutions for the disadvantages in these processes, such as high temperatures, large amounts of waste and toxic, volatile solvents, ILs appear to be a promising reaction medium.

The underlying idea of the application of ILs and DESs for metal oxide processing is a two-step process, as shown in Figure 2. First, metal oxides are dissolved in the IL or DES at relatively low temperatures. Second, proceeding from the obtained solution, either metal compounds are synthesised via downstream chemistry or metals are electrochemically deposited. Regarding the sustainability of such processes, the recyclability of the ILs is highly desirable. Despite a lot of research has been performed on metal extraction using ILs, a large number of these reports assumes metal ions dissolved in and extracted from different solvents [97–100]. The direct dissolution of metal oxides by ILs, however, appears to be considerably less investigated. Despite the topic was addressed in some review articles [22,23], it was covered rather secondarily. A more comprehensive summary on the dissolution of metal oxides in ILs is given in the following section. Detailed information about the dissolution of specific metal oxides in different ILs is listed in Table 2.

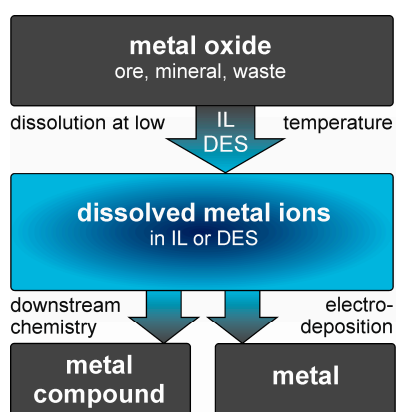


Figure 2. Scheme of the general idea of metal oxide processing in ILs and DESs.

Table 2. Overview about metal oxides dissolved in different ILs as well as corresponding references.

Metal Oxide	Solvent	Reference
Ag ₂ O	[bmim]Cl	[101]
	[emim][SCN]	[101]
	[emim][dca]	[101]
	[emim][OAc]	[101]
Al ₂ O ₃	[Hbet][NTf ₂]/H ₂ O and derivatives	[102–104]
	[NRRRC ₃ SO ₃ H][NTf ₂]/H ₂ O	[105]
BaO	[PRRRC ₃ SO ₃ H][NTf ₂]/H ₂ O	[105]
	[Hbet][NTf ₂]	[106]
Bi ₂ O ₃	[Hbet] ₂ [NTf ₂]Cl	[106]
	[bpyr]Cl/AlCl ₃	[107]
CaO	[Hbet][NTf ₂]	[106]
	[Hbet] ₂ [NTf ₂]Cl	[106]
	[P ₆₆₆₁₄]Cl/aq. HCl	[108]
CdO	[Hbet][NTf ₂]	[106]
	[Hbet] ₂ [NTf ₂]Cl	[106]
CoO	[N ₁₁₁ C ₂ OSO ₃ H][NTf ₂]/H ₂ O	[109]
	[Hbet][NTf ₂]/H ₂ O and derivatives	[102,104]
Co ₃ O ₄	[P ₆₆₆₁₄]Cl/aq. HCl	[108]
	[NRRRC ₃ SO ₃ H][NTf ₂]/H ₂ O	[105]
	[PRRRC ₃ SO ₃ H][NTf ₂]/H ₂ O	[105]
Cr ₂ O ₃	[Hbet][NTf ₂]	[106]
	[Hbet] ₂ [NTf ₂]Cl	[106]
	[NRRRSO ₃ H][NTf ₂]/H ₂ O	[105]
	[PRRRSO ₃ H][NTf ₂]/H ₂ O	[105]
Cu ₂ O	[NRRRH–SO ₃ H][NTf ₂]/[emim]Cl	[110]
	[N ₁₁₁ C ₂ OSO ₃ H][NTf ₂]/H ₂ O	[109]
CuO	[NRRRC ₃ SO ₃ H][NTf ₂]/H ₂ O	[105]
	[PRRRC ₃ SO ₃ H][NTf ₂]/H ₂ O	[105]
	[Hbet][NTf ₂]	[106]
	[Hbet] ₂ [NTf ₂]Cl	[106]
Dy ₂ O ₃	[P ₆₆₆₁₄]Cl/aq. HCl	[108]
	[emim]Cl	[101]
	[emim][OAc]	[101]
	[Hbet][NTf ₂]/H ₂ O and derivatives	[102,104]
Er ₂ O ₃	[Hbet][NTf ₂]	[106]
	[Hbet] ₂ [NTf ₂]Cl	[106]
	[NRRRC ₃ SO ₃ H][NTf ₂]/H ₂ O	[105]
	[PRRRC ₃ SO ₃ H][NTf ₂]/H ₂ O	[105]
Eu ₂ O ₃	[NRRRH–SO ₃ H][NTf ₂]/[emim]Cl	[110]
	[N ₁₁₁ C ₂ OSO ₃ H][NTf ₂]/H ₂ O	[109]
Fe ₂ O ₃	[Hbet][NTf ₂]/H ₂ O and derivatives	[102,104]
	[bmim][NTf ₂]/aq. HNO ₃	[111]
Gd ₂ O ₃	[Hbet][NTf ₂]/H ₂ O and derivatives	[102,104]
	[P ₆₆₆₁₄]Cl/aq. HCl	[108]
	[Hbet] ₂ [NTf ₂]Cl	[106]
	[NRRRC ₃ SO ₃ H][NTf ₂]/H ₂ O	[105]
HgO	[PRRRC ₃ SO ₃ H][NTf ₂]/H ₂ O	[105]
	[NRRRH–SO ₃ H][NTf ₂]/[emim]Cl	[110]
Ho ₂ O ₃	[N ₁₁₁ C ₂ OSO ₃ H][NTf ₂]/H ₂ O	[109]
	[Hbet][NTf ₂]/H ₂ O and derivatives	[102,104]
La ₂ O ₃	[Hbet][NTf ₂]/H ₂ O and derivatives	[102,104]
	[NRRRC ₃ SO ₃ H][NTf ₂]/H ₂ O	[105]
	[PRRRC ₃ SO ₃ H][NTf ₂]/H ₂ O	[105]
	[NRRRH–SO ₃ H][NTf ₂]/[emim]Cl	[110]
	[N ₁₁₁ C ₂ OSO ₃ H][NTf ₂]/H ₂ O	[109]

Table 2. Cont.

Metal Oxide	Solvent	Reference
Li ₂ O	Ethylene carbonate/AlCl ₃	[112]
Lu ₂ O ₃	[Hbet][NTf ₂]/H ₂ O and derivatives	[102,104]
MgO	[Hbet] ₂ [NTf ₂]	[106]
	[Hbet] ₂ [NTf ₂]Cl	[106]
	[P ₆₆₆₁₄]Cl/aq. HCl	[108]
	[Hbet][NTf ₂]/H ₂ O	[102,103]
MnO	[Hbet][NTf ₂]	[106]
	[Hbet] ₂ [NTf ₂]Cl	[106]
	[NRRRC ₃ SO ₃ H][NTf ₂]/H ₂ O	[105]
	[PRRRC ₃ SO ₃ H][NTf ₂]/H ₂ O	[105]
	[NRRH-SO ₃ H][NTf ₂]/[emim]Cl	[110]
MnO ₂	[Hbet] ₂ [NTf ₂]Cl	[106]
	[NRRH-SO ₃ H][NTf ₂]/[emim]Cl	[110]
MoO ₃	[Hbet][NTf ₂]	[106]
	[Hbet] ₂ [NTf ₂]Cl	[106]
Nd ₂ O ₃	[bmim][NTf ₂]/aq. HNO ₃	[111]
	[Hbet][NTf ₂]/H ₂ O and derivatives	[102,104]
	[NRRRC ₃ SO ₃ H][NTf ₂]/H ₂ O	[105]
	[PRRRC ₃ SO ₃ H][NTf ₂]/H ₂ O	[105]
	[NRRH-SO ₃ H][NTf ₂]/[emim]Cl	[110]
	[N ₁₁₁ C ₂ OSO ₃ H][NTf ₂]/H ₂ O	[109]
	[P ₆₆₆₁₄]Cl/aq. HCl	[108]
	[emim]Cl	[101]
[emim][OAc]	[101]	
NiO	[Hbet][NTf ₂]/H ₂ O and derivatives	[102–104]
	[Hbet] ₂ [NTf ₂]Cl	[106]
	[NRRRC ₃ SO ₃ H][NTf ₂]/H ₂ O	[105]
	[PRRRC ₃ SO ₃ H][NTf ₂]/H ₂ O	[105]
	[NRRH-SO ₃ H][NTf ₂]/[emim]Cl	[110]
[N ₁₁₁ C ₂ OSO ₃ H][NTf ₂]/H ₂ O	[109]	
PbO	[Hbet][NTf ₂]/H ₂ O and derivatives	[103,104,113]
	[Hbet][NTf ₂]	[106]
	[Hbet] ₂ [NTf ₂]Cl	[106]
PbO ₂	[Hbet][NTf ₂]/H ₂ O	[113]
	[Hbet][NTf ₂]	[106]
PdO	[Hbet] ₂ [NTf ₂]Cl	[106]
	[Hbet][NTf ₂]/H ₂ O and derivatives	[102,104]
Pr ₆ O ₁₁	[bmim][NTf ₂]/aq. HNO ₃	[111]
	[Hbet][NTf ₂]/H ₂ O and derivatives	[104,114]
PuO ₂	[Hbet][NTf ₂]/H ₂ O	[18]
Sc ₂ O ₃	Derivates of [Hbet][NTf ₂]/H ₂ O	[104]
Sm ₂ O ₃	[Hbet][NTf ₂]/H ₂ O and derivatives	[102,104]
	[Hbet] ₂ [NTf ₂]Cl	[106]
SnO	[Hbet][NTf ₂]	[106]
	[Hbet] ₂ [NTf ₂]Cl	[106]
SrO	[Hbet][NTf ₂]	[106]
	[Hbet] ₂ [NTf ₂]Cl	[106]
Tb ₄ O ₇	[Hbet][NTf ₂]/H ₂ O and derivatives	[102,104]
ThO ₂	[Hbet] ₂ [NTf ₂]Cl	[106]
	[NRRRC ₃ SO ₃ H][NTf ₂]/H ₂ O	[105]
TiO ₂	[PRRRC ₃ SO ₃ H][NTf ₂]/H ₂ O	[105]
	[Hbet][NTf ₂]/H ₂ O and derivatives	[102,104]
Tm ₂ O ₃	[emim]Cl/FeCl ₃	[115]
	[bmim]Cl/FeCl ₃	[115]
	[bdmim]Cl/FeCl ₃	[115]
	[bmim][NTf ₂]/aq. HNO ₃	[111]
	[emim][F(HF) _n] (n = 2, 3)	[116]
UO ₂	[Hbet][NTf ₂]/H ₂ O	[117]
	[emim]Cl/AlCl ₃	[118]
	[pdmim]Cl/AlCl ₃	[118]
	[bmim][NTf ₂]/aq. HNO ₃	[111]
	[dmah][NTf ₂]	[119]
UO ₃	[emim][F(HF) _n] (n = 2, 3)	[116]
	[Hbet][NTf ₂]/H ₂ O and derivatives	[102,104,117,120]

Table 2. Cont.

Metal Oxide	Solvent	Reference
V ₂ O ₃	[Hbet][NTf ₂]	[106]
	[Hbet] ₂ [NTf ₂]Cl	[106]
	[emim]Cl/AlCl ₃	[121]
V ₂ O ₅	[bmim]Cl/AlCl ₃	[121]
	[bpyr]Cl/AlCl ₃	[107]
	[Hbet][NTf ₂]	[106]
Y ₂ O ₃	[Hbet] ₂ [NTf ₂]Cl	[106]
	[Hbet][NTf ₂]/H ₂ O and derivatives	[102,104]
	[NRRRC ₃ SO ₃ H][NTf ₂]/H ₂ O	[105]
Yb ₂ O ₃	[PRRRC ₃ SO ₃ H][NTf ₂]/H ₂ O	[105]
	[Hbet][NTf ₂]/H ₂ O and derivatives	[102,104]
WO ₃	[NRRRC ₃ SO ₃ H][NTf ₂]/H ₂ O	[105]
	[PRRRC ₃ SO ₃ H][NTf ₂]/H ₂ O	[105]
ZnO	[P ₆₆₆₁₄]Cl/aq. HCl	[108]
	[emim]Cl	[101]
	[emim][OAc]	[101]
	[omim][OTf]	[122]
	[Hbet][NTf ₂]/H ₂ O and derivatives	[102–104]
	[Hbet][NTf ₂]	[106]
ZnO	[Hbet] ₂ [NTf ₂]Cl	[106]
	[NRRRC ₃ SO ₃ H][NTf ₂]/H ₂ O	[105]
	[PRRRC ₃ SO ₃ H][NTf ₂]/H ₂ O	[105]
	[NRRH-SO ₃ H][NTf ₂]/[emim]Cl	[110]

3.1.1. Chloridometalate ILs

First experiments on the dissolution of metal oxides have been performed in chloridoaluminate ILs, consisting of a chloride salt with a large organic cation and AlCl₃. Depending on the molar ratio of these components, basic, neutral and acidic ILs are distinguished. The IL is considered basic with an excess of the organic chloride salt and acidic with an excess of AlCl₃, while neutral ILs consist of an equimolar amount of both, i.e., [AlCl₄][−]. Because of the hygroscopy of AlCl₃, all experiments have to be performed under inert gas atmosphere [19].

Dissolution experiments have especially been performed in Lewis-basic ILs, as the presence of free chloride anions appears important for the formation of soluble complex anions. Thus, Dai et al. dissolved UO₃ in basic ILs of [emim]Cl or [pdmim]Cl and AlCl₃. Furthermore, a connection between the ability of the IL cation to form hydrogen bonds and the solubility of UO₃ can be drawn, as higher solubilities are found in the [emim]⁺ IL with a hydrogen atom at C2. The favoured formation of the stable [UO₂Cl₄]^{2−} complex anion [118] was shown by molecular dynamics studies by Chaumont and Wipff [123].

A wider range of Lewis acidity was covered by the studies of V₂O₅ in acidic, neutral and basic [emim]Cl/AlCl₃ and [bmim]Cl/AlCl₃ by Bell and Castleman. They reported the formation of VO₂Cl₂[−] and metavanadates [(VO₃)_n]^{n−} (n = 3, 4) as main species with their ratio being dependent on the acidity of the IL and the concentration of V₂O₅. Furthermore, in acidic melts, the reaction of these species with Al₂O₇[−] is assumed, yielding volatile VOCl₃. In contrast to that, no dissolution was observed for ILs with weakly-coordinating anions, such as [bmim][BF₄] and [bmim][OTf]. This highlights the importance of strong interactions between the IL and the metal oxide, necessary to overcome the lattice energy of the solid [121].

V₂O₅ as well as Bi₂O₃ were also dissolved in the neutral IL [bpyr]Cl/AlCl₃ by Mahjoor and Lattuner. Upon dissolution, the chlorination of the metal atoms takes place yielding the complex anions [V₄O₄Cl₁₂]^{4−} and [Bi₄Cl₁₆]^{4−} [107].

Shi et al. dissolved Li₂O in the Lewis-basic IL ethylene carbonate/AlCl₃. They suggest the strong coordination power of the hypothetical [AlCl₂]⁺ cation as driving force for the dissolution of Li₂O. Differing from the previous ILs, instead of tetrachloridoaluminate, in this IL, [AlCl₂(ethylene

carbonate)₄]⁺ complexes are formed. Subsequently, the ligand exchange between ethylene carbonate and Li₂O causes the dissolution [112].

Similar to aluminium, also iron appears to be a suitable addition to an IL for the dissolution of UO₂, as Yao and Chu showed. They reported the oxidation, hence dissolution, of the metal oxide to UO₂²⁺ in mixtures of imidazolium-based, iron-containing ILs and their corresponding imidazolium chloride IL. In the course of this, [FeCl₄][−] is reduced to [FeCl₄]^{2−} [115]. This implies that the same IL cannot be reused for the dissolution of UO₂ without previous oxidising workup.

Deducing from these reports, chloridometalate ILs can be suitable solvents for the dissolution of metal oxides as they provide strong interactions to the metal atom of the metal oxide. In most cases, chloride ions play a vital role as strong ligands in the resulting coordination sphere. However, a large drawback of this kind of IL is their water and air sensitivity, requiring expensive inert gas atmosphere set-ups and complicating up-scaling.

3.1.2. Air- and Water-Stable ILs

In order to overcome the disadvantages of chloridometalate ILs, further research on the dissolution of metal oxides in ILs focused on the application of different ILs with discrete anions. They allow an experimental set-up under ambient conditions and the application of aqueous additives. As such anions often are merely weakly coordinating, the interactions necessary for the dissolution of metal oxides, are provided by the cations in most cases.

As the oxygen anion of a metal oxide is too unstable to exist in a free form, an obvious approach could be its transfer into stable compounds, thereby dissolving the metal ions. Hence, protons could be provided for the reaction to water. In water-stable ILs, aqueous acids can easily be added for this purpose, as Binnemans et al. showed. They dissolved CaO, CoO, CuO, Fe₂O₃, MnO, NiO and ZnO in the acid-saturated IL [P₆₆₆₁₄]Cl (10 wt % 12 M HCl), whereas the respective tetrachloridometalate anions formed, except for calcium, where a partly hydration is assumed. Indeed, by this method metal oxides were directly dissolved into an IL phase, however, the solubility is similar to pure hydrochloric acid [108].

Similarly, Billard et al. dissolved Eu₂O₃, Nd₂O₃, Pr₆O₁₁, UO₂ and UO₃, in a mixture of [bmim][NTf₂] and small amounts aqueous nitric acid (14 M). For uranium, UO₂(NO₃)₃[−] was identified as an ionic species present in the solution, revealing the oxidation of UO₂ by the reduction of NO₃[−] to NO₂[−]. They, furthermore, reported a reaction-promoting effect of water, as the dissociation of nitric acid might be supported [111].

Instead of adding mineral acids, Moyer et al. used the acidic IL [dmah][NTf₂] for the dissolution of UO₃. The [dmah]⁺ cation is assumed to dissociate in a proton and the corresponding base which is suitable to solvate the uranyl ion. Apparently, the water evolving during the reaction has a reaction-promoting effect by supporting the dissociation of [dmah]⁺. [emim][NTf₂] turned out to be a suitable inert additive for dilution in order to lower the viscosity for subsequent electrochemical experiments [119]. Despite the IL cation directly acting as a reactant in the reaction, it should be possible to recover it by addition of an acid, hence protonation. Thus, the metal ions could be transferred to another phase and the IL recycled.

Similarly, Binnemans et al. made use of the acidic proton at the C2 position in imidazolium cations. Thus, they demonstrated the solubility of Ag₂O, CuO, NiO and ZnO in several imidazolium-based ILs via the coordination of carbene ligands. The deprotonation of C2 and the subsequent carbene formation appear to be the driving force of the metal oxide dissolution [101], as a suitable ligand for the metal cation is provided.

Also using the coordinating abilities of the IL's cation, Endres et al. applied the IL [mim][OTf] for the dissolution of ZnO. Zinc(II) is assumed to be chelated by 1-methylimidazole via the nitrogen atoms. Furthermore, Zn–O interactions are proposed with the [OTf][−] anion as well as with water molecules [122].

Applying a rather uncommon anion, Zarzana et al. dissolved UO_2 and UO_3 in the IL [emim][F(HF) $_n$] ($n = 2, 3$). This IL exhibits a significant fluorinating ability, promoting the dissolution of metal oxides. The dissolved species for UO_2 is assumed to be UF_6^- at first, which is further oxidised to uranium(VI) by oxygen from air. Upon this process, the diffusion of oxygen into the solution takes place, yielding uranyl fluoride species [116]. This IL should rather be perceived as a fluorinating agent than as a solvent for metal oxides, as the dissolution process involves the consumption of the IL anion. Hence, recyclability is limited.

Using air- and water-stable ILs, naturally simplifies experimental works. However, the strong interactions to the metal oxide's cation, which tetrachloridometalate ILs offer, have to be provided in another way, in order to dissolve metal oxides. Mostly, this is achieved by cations featuring electron-rich atoms acting as ligand. Furthermore, it appears reasonable to provide protons for the reaction with oxygen. This could be a driving force for the reaction, according to Le Châtelier's principle.

3.1.3. Task-Specific ILs

Large progress in the dissolution of metal oxides was made by the application of task-specific ILs (TSILs), featuring a functional group, a carboxyl group, at the cation. Brønsted-acidic groups combine both advantages already attempted in common water-stable ILs: On one side, protons are suitable to form water with the oxygen atom of the metal oxide, on the other, the remaining, electron-rich functional group is a suitable ligand for the metal ions. Figure 3 gives an overview about the Brønsted acidic TSIL discussed in this review.

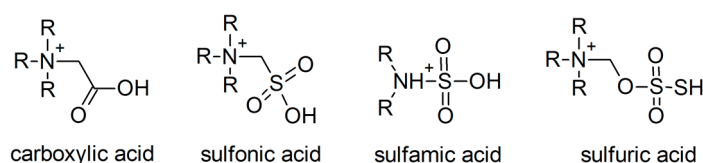


Figure 3. Overview of Brønsted acidic task-specific ILs (TSIL) cations. The picture shows the simplest representative of each kind of IL as variation in the length of the alkyl chain between the ammonium and the acidic functional groups are possible.

As an example for carboxyl-functionalised ILs, a lot of research has been performed using the IL [Hbet][NTf $_2$], first described by Binnemans et al. [102]. After the water-forming reaction of acidic betinium protons with oxide atoms from the metal oxide, the remaining betaine molecule coordinates to the metal cation to form metal-betaine complexes, as shown in Figure 4.

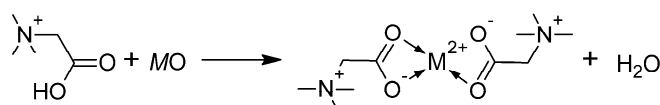


Figure 4. Dissolution mechanism of a metal oxide in [Hbet][NTf $_2$].

As betaine is too sterically demanding to saturate all coordination sites, smaller molecules are necessary in order to promote dissolution. Therefore, all reactions were performed in aqueous solutions, thus providing aqua ligands. Although numerous crystal structures of polymeric metal-betaine-aqua complexes were described [102,103], synchrotron techniques revealed a dissociation to the monomeric complexes in solution [114]. A large number of oxides of main and subgroup as well as lanthanide and actinide metals were dissolved in aqueous [Hbet][NTf $_2$] [18,102,103,113,114,117,124,125], however, negligible dissolution was observed for not readily soluble, more covalent metal oxides, such as Al_2O_3 [102,126,127], Fe_2O_3 (haematite) [126,127], MnO_2 [102], TiO_2 (anatase-rutile) [127], cobalt oxides [102] and U_3O_8 [117].

Furthermore, Nockemann et al. and Binnemans et al. reported several TSILs similar to [Hbet][NTf₂] with a carboxyl group at the cation and a [NTf₂][−] anion suitable for the dissolution of metal oxides [103,120]. For another aqueous carboxyl functionalised IL, 3-(5-carboxypropyl)-1-methylimidazolium bromide, Li et al. found a good solubility of Eu₂O₃ [128].

Gupta, Chandrakumar et al. showed that the addition of water as a solvent is not necessary in order to obtain metal-betaine-water complexes, but the water evolving during the reaction is sufficient when refluxed [18].

It has to be taken into account, that some metal oxides undergo redox reactions upon dissolution. This might involve a partly decomposition of the IL. Chen et al. found evidence for the reduction of Pb⁴⁺ from PbO₂ to Pb²⁺ in [Hbet][NTf₂]. The same complex [Pb(bet)₂(H₂O)₂]²⁺ is formed from PbO₂ and PbO [113]. For the dissolution of UO₂, Nagarajan et al. identified the oxidation to UO₂²⁺ as crucial [117].

Furthermore, aqueous [Hbet][NTf₂] was applied to natural mixtures of substances for the leaching of specific metals from recycling waste. Thus, Davris et al. leached rare earth metals from bauxite residues. A good selectivity for rare earth metals, and, therefore, the dissolution of their oxides, was found against iron (haematite), aluminium, titanium (anatase, rutile) and silicon. Also scandium showed a minor solubility [127].

An optimisation of the scandium leaching conditions in this IL regarding the reaction temperature and the molar ratio of the reagents was performed by Mawire and van Dyk [129]. Furthermore, Grimes et al. found that by changing the reaction temperature and the IL-water ratio of aqueous [Hbet][NTf₂], the relative solubility of rare earths can be adjusted, thus enabling the separation of light (Eu₂O₃, La₂O₃, Nd₂O₃) from heavy rare earths (Y₂O₃, Yb₂O₃) and Gd₂O₃ [130].

[Hbet][NTf₂] was also employed for the recycling of fluorescent lamp phosphor waste by Dupont and Binnemans. They selectively dissolved europium doped Y₂O₃ as the IL, in contrast to mineral acids, is not able to efficiently dissolve non-oxygen anions [131].

The group of Binnemans also used aqueous [Hbet][NTf₂] to leach neodymium, cobalt and dysprosium from roasted NdFeB magnets at 80 °C, while iron (haematite) remained almost completely undissolved [124].

These examples demonstrate that, on one side, the dissolution characteristics of [Hbet][NTf₂] can be utilised for specific tasks. Thus, the negligible dissolution of non-oxidic salts as well as covalent oxides, such as Al₂O₃, Fe₂O₃, TiO₂ and SiO₂, enables the separation of metal oxides. On the other, it becomes apparent that the ability of [Hbet][NTf₂] to dissolve metal oxides is tuneable by varying reaction parameters. Further investigations in this field could reveal new, efficient ways for the separation of metal oxides from starting materials of diverse composition.

The leaching experiments from NdFeB magnets by Binnemans et al. were repeated in water-free [Hbet][NTf₂] at 175 °C in a system open to the air, in order to allow the evaporation of water [132]. The absence of water could be advantageous for the further processing of the dissolved metal ions: On one side, it might prove difficult to leach the metal cations from their aqua-complexes for downstream chemistry, on the other, the presence of water might complicate a subsequent electrolysis of the dissolved metals. However, in the approach of Binnemans et al. a significant increase in the reaction time as well as a decrease in the coordination number of the metal ions was found. Because of the steric demands of betaine, not all coordination sites can be occupied. However, a first experiment showed, that chloride as additional, smaller ligand promotes the dissolution of CuO in the absence of water [132].

Pursuing this water-free approach, we recently published a comprehensive investigation on the dissolution of 30 metal oxides in water-free [Hbet][NTf₂]. For the example of CuO, the crystal structure of the water-free copper-betaine complex was solved, as shown in Figure 5. Apparently, in the absence of stronger small ligands, free coordination sites can be occupied by the weakly coordinating [NTf₂][−] anion. Indeed, a positive effect of water on the dissolution was confirmed, but by the addition of [Hbet]Cl, thus providing chloride as additional, nucleophilic ligand in the IL [Hbet]₂[NTf₂]Cl,

significantly more metal oxides can be dissolved in the IL, including quite unreactive metal oxides, such as Fe_2O_3 (haematite), MnO_2 (pyrolusite) and ThO_2 . However, under the chosen conditions, chloride ions cause a partly decomposition of the IL [106]. Similar to the previously discussed separation experiments, the optimisation of the reaction parameters, such as reaction temperature and duration, as well as chloride concentration could enable the avoidance of this effect.

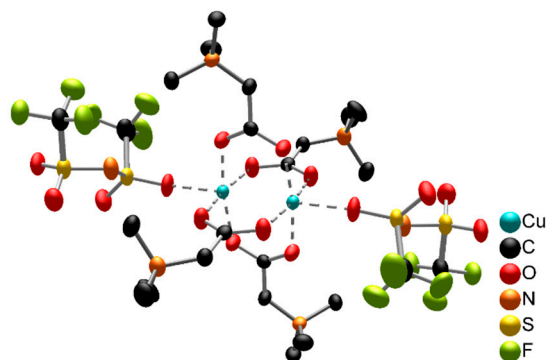


Figure 5. The water-free metal-betaine complex $[\text{Cu}_2(\text{bet})_4(\text{NTf}_2)_2]^{2+}$ obtained by the dissolution of CuO in $[\text{Hbet}][\text{NTf}_2]$. Coordinative interactions are marked as dotted lines. The ellipsoids enclose 70% of the probability density of the atoms at 100 K. H atoms are omitted for clarity.

While the so far mentioned studies were of rather empiric nature, Qin et al. previously had suggested an U/x value of a metal oxide M_xO_y (U = lattice energy) to predict the solubility of metal oxides. This theory was based on dissolution experiments with numerous f-block elements as well as divalent metal oxides. It underlines the correlation between the lattice energy of a metal oxide and its solubility [125]. However, our findings show that this assumption is not valid for all metal oxides, which is in agreement with the report by Gupta, Chandrakumar et al. who dissolved PuO_2 [18], despite predicted insoluble by Qin et al. [125]. Apparently, the lattice energy is not the only factor influencing the solubility, but also other parameters, such as reaction conditions [18] and crystal phase are important. As the dissolution of metal oxides in $[\text{Hbet}][\text{NTf}_2]$ comes down to an acid-base reaction, we consider especially the basicity of the metal oxide to be significant. Hence, for example, a very good solubility is found for alkaline earth metal oxides [106]. However, because of the lack of quantitative data about the basicity of different metal oxides, a validation of this assumption and the exact prediction of dissolution behaviour is not possible, yet.

Making inert metal oxides accessible for dissolution, more acidic IL cations with a sulfonic acid functional group could be applied, as Binnemans et al. reported. Thus in a 1:1 mixture of different sulfonic acid functionalised ILs and water, stoichiometric amounts of cobalt oxides, Fe_2O_3 and smaller amounts of Al_2O_3 , Cr_2O_3 , TiO_2 and WO_3 were dissolved at 80 °C [105]. Other ILs with sulfamic or alkylsulfuric acid functional groups at the cation show a similar or even higher acidity and some dissolution ability for rather unreactive metal oxides [109,110]. Furthermore, the addition of $[\text{emim}]\text{Cl}$ was found to support the dissolution because of the good solvating ability of the chloride ions [110].

The application of Brønsted-acid-functionalised ILs could make numerous metal oxides accessible for dissolution. Even rather inert metal oxides could be dissolved in increasingly acidic ILs, highlighting the importance of understanding the nature of the acid-base reaction taking place. Several studies of reaction parameters also show, that no absolute statements about an IL dissolving a metal oxide are possible. Instead, always reaction conditions and the composition of the sample have to be taken into account. However, the underlying causes for these effects are not understood, yet. Systematic studies could help to clarify the processes taking place. An advantage of such Brønsted-acidic ILs is that they allow the recycling of the IL. Because of the corresponding base acting as ligand coordinating metal ions, the IL cation is easily retrievable by protonation while the metal ions are leached into another phase.

3.1.4. Conclusion on Metal Oxide Dissolution in ILs

The ability of ILs to dissolve metal oxides results from the coordination abilities of either the cations or anions. Strong nucleophiles, such as chloride, fluoride, carbene or chelating functional groups are suitable ligands. However, task-specific ILs with Brønsted acidic functional groups appear to be especially suitable for the dissolution of metal oxides. The underlying cause is the driving force of the reaction of the protons with the oxygen atoms forming water. The resulting negatively charged functional group, subsequently, is able to act as a chelating ligand, thus, providing relatively strong interactions to the metal cations. Hence, even not readily dissolvable metal oxides exhibit some solubility in these ILs.

Despite one IL fluorinating metal cations via the anion and tetrachloridometalate ILs, dissolution mechanisms appear to sum up to coordinating interactions between the IL cation and metal ions. Anions rather influence these reactions by providing the IL with suitable properties, such as a low melting point, a low viscosity and, possibly, stability towards air and moisture. Especially the very weakly coordinating, bulky anion $[\text{NTf}_2]^-$ is used in most ILs for dissolution studies, thus relying on strongly interacting cations. For the example of $[\text{Hbet}][\text{NTf}_2]$, other common anions give compounds with melting points well above 100 °C and, therefore, per definition no ILs. However, the complex compound $[\text{Cu}_2(\text{bet})_4(\text{NTf}_2)_2]^{2+}$ shows, that this anion can also act as a ligand in the metal ion's coordination sphere if no stronger ligands are present.

An interesting connection between the acidity of the IL cation and the ability to dissolve not readily soluble metal oxides becomes apparent. The development of new ILs with special regard to the acidity might allow the dissolution of even more metal oxides. On the other side, the dissolution of metal oxides seems to be tuneable by changing the reaction parameters, which is another promising starting point for systematic future research.

Furthermore, by varying reaction parameters as well as by the application of different ILs, new processes for the segregation of different metal oxides at low temperatures and with smaller amounts of waste might be achievable. In order to design economical as well as sustainable processes, further research should also focus on the recyclability of the IL. Several reports have shown, that the recycling of the IL is possible, next steps should include the design of efficient, maybe even up-scaled processes.

3.2. Dissolution in DESs

Some amount of work on the dissolution of metal oxides has also been performed in DESs, although research seems to have had a focus on ILs. Featuring the advantages of lower costs and less toxicity because of various naturally available components, the dissolution process appears to add up to the same principle like in ILs; the presence of coordinating ligands that are able to interact with the metal cations. Nevertheless, there are mechanistic ambiguities that should be resolved by further research. An overview about the metal oxides dissolved in different DESs is given in Table 3.

Table 3. Overview about metal oxides dissolved in different DESs as well as corresponding references.

Metal Oxide	Solvent	Reference
CoO	Choline chloride-malonic acid (1:1)	[133]
Co ₃ O ₄	Choline chloride-malonic acid (1:1)	[133]
	Choline chloride- <i>p</i> -toluenesulfonic acid (1:2; 1:2; 2:1)	[134]
CrO ₃	Choline chloride-urea (1:2)	[133]
	Choline chloride-malonic acid (1:1)	[133]
	Choline chloride-urea (1:2)	[133,135,136]
Cu ₂ O	Choline chloride-malonic acid (1:1)	[133]
	Choline chloride-ethylene glycol (1:2)	[133]
	Choline chloride- <i>p</i> -toluenesulfonic acid (1:2; 1:2; 2:1)	[134]

Table 3. Cont.

Metal Oxide	Solvent	Reference
CuO	Choline chloride-urea (1:2)	[135,137]
	Choline chloride-malonic acid (1:1)	[133,138]
	Choline chloride-oxalic acid (1:1)	[138]
	Choline chloride-phenylpropionic acid (1:2)	[138]
	Choline chloride- <i>p</i> -toluenesulfonic acid (1:2; 1:2; 2:1)	[134]
Eu ₂ O ₃	Ethylene glycol-maleic acid (1:1; 2:1; 4:1; 6:1)	[139]
	Ethylene glycol-citric acid (4:1)	[139]
	1,2-Propanediol-maleic acid (4:1)	[139]
	Glycerol-maleic acid (4:1)	[139]
FeO	1,4-Butanediol-maleic acid (4:1)	[139]
	Choline chloride-malonic acid (1:1)	[133]
Fe ₂ O ₃	Choline chloride-malonic acid (1:1)	[133]
	Choline chloride- <i>p</i> -toluenesulfonic acid (1:2; 1:2; 2:1)	[134]
Fe ₃ O ₄	Choline chloride-malonic acid (1:1)	[133,138]
	Choline chloride-oxalic acid (1:1)	[138]
	Choline chloride-phenylpropionic acid (1:2)	[138]
Gd ₂ O ₃	Choline chloride- <i>p</i> -toluenesulfonic acid (1:2; 1:2; 2:1)	[134]
	Ethylene glycol-maleic acid (4:1)	[139]
In ₂ O ₃	Choline chloride- <i>p</i> -toluenesulfonic acid (1:2; 1:2; 2:1)	[134]
	Ethylene glycol-maleic acid (1:1; 2:1; 4:1; 6:1)	[139]
La ₂ O ₃	Ethylene glycol-citric acid (4:1)	[139]
	1,2-Propanediol-maleic acid (4:1)	[139]
	Glycerol-maleic acid (4:1)	[139]
MnO	Choline chloride-malonic acid (1:1)	[133]
	Choline chloride- <i>p</i> -toluenesulfonic acid (1:2; 1:2; 2:1)	[134]
Mn ₂ O ₃	Choline chloride-malonic acid (1:1)	[133]
	Choline chloride-urea (1:2)	[135]
MnO ₂	Choline chloride-malonic acid (1:1)	[133]
	Choline chloride- <i>p</i> -toluenesulfonic acid (1:2; 1:2; 2:1)	[134]
MoO ₃	Choline chloride-urea (1:2)	[140]
Nd ₂ O ₃	Ethylene glycol-maleic acid (4:1)	[139]
	Choline chloride-urea (1:2)	[135]
NiO	Choline chloride-malonic acid (1:1)	[133]
Ni ₂ O ₃	Choline chloride-urea (1:2)	[141]
PbO	Choline chloride-urea (1:2)	[142–144]
	Choline chloride-urea (1:2)	[135]
PbO ₂	Choline chloride- <i>p</i> -toluenesulfonic acid (1:2; 1:2; 2:1)	[134]
	Ethylene glycol-maleic acid (4:1)	[139]
Pr ₆ O ₁₁	Ethylene glycol-maleic acid (4:1)	[139]
Sm ₂ O ₃	Ethylene glycol-maleic acid (4:1)	[139]
	Choline chloride-urea (1:2)	[133]
	Choline chloride-malonic acid (1:1)	[133]
V ₂ O ₃	Choline chloride-ethylene glycol (1:2)	[133]
	Choline chloride-urea (1:2)	[133,145]
	Choline chloride-malonic acid (1:1)	[133]
V ₂ O ₅	Choline chloride-ethylene glycol (1:2)	[133]
	Choline chloride-urea (1:2)	[133,135,137,146,147]
	Choline chloride-malonic acid (1:1)	[133,138]
	Choline chloride-oxalic acid (1:1)	[138]
	Choline chloride-phenylpropionic acid (1:2)	[138]
ZnO	Choline chloride-ethylene glycol (1:2)	[133]
	Choline chloride- <i>p</i> -toluenesulfonic acid (1:2; 1:2; 2:1)	[134]
	[bmim]Cl-urea (1:1; 1:2)	[148,149]
	[emim]Cl-urea (1:1; 1:2)	[149,150]
	[amim]Cl-urea (1:1)	[149]

3.2.1. Choline Chloride-Urea

Early dissolution experiments were performed in the popular DES choline chloride-urea (molar ratio 1:2) by suspending the reagents at temperatures below 100 °C in order to avoid the decomposition of urea. The driving force of dissolution is the coordination of urea to the metal atom [135,140]. This is supported by DFT calculations performed by Rimsza and Corrales. They showed that the favoured complex for CuO is [Cu(urea)]²⁺ with urea in the neutral molecular state [151].

For several easily soluble metal oxides, such as copper oxides [136,137], PbO [142–144] or ZnO [137,146–150], various DESs appear to be excellent solvents. Hence, their dissolution, to date, is kind of a chemical routine during the preparation of samples for electrochemical experiments.

Furthermore, Davies et al. found a medium solubility for, MnO₂ and NiO, but negligible solubility for Al₂O₃, CaO and iron oxides. Despite, interestingly, some dissolution was found for the rather inert MnO₂, an authentic sample of steel furnace waste showed that because of the significantly better solubility of zinc and lead oxides, their selective dissolution is possible [135].

Furthermore, Huang and Zhang showed the dissolution of Ni₂O₃ [141], Al-Hajri et al. dissolved MoO₃ [140] and Antal et al. reported a high solubility of V₂O₅, yielding the high-valent, stable [H₂V₁₀O₂₈]^{4−} complex anion. Because of a distinct hydrogen bond network, the slow crystallisation of the compound [(CH₃)₃N(CH₂)₂OH]₄[H₂V₁₀O₂₈]·2(NH₂)₂CO occurs within several months [145].

Indeed, urea is able to coordinate to metal atoms, however, usually it acts as a monodentate ligand via the oxygen atom, thus, not offering very strong interactions. However, the few experiments performed with this DES do not allow any general conclusions.

3.2.2. Acidic DESs

Further studies with regard to the importance of the acidity of DESs were performed in mixtures of choline chloride and organic acids below 100 °C. Abbott et al. dissolved CuO, Fe₃O₄ and ZnO, in DESs of choline chloride and malonic, oxalic or phenylpropionic acid. All oxides were dissolved to a significant extent, however, the solubility varies in the different DESs without any cause being identifiable [138].

In another study, the group showed that malonic acid-based choline chloride DESs (molar ratio 1:1) have a higher solubility of metal oxides than the ones based on urea and ethylene glycol (molar ratio 1:2). This is attributed to the presence of protons acting as oxygen acceptor and, thus, promoting dissolution. Again, the correlation showed that more ionic oxides show a higher solubility in the examined DESs, while the dissolution of more covalent oxides is negligible. However, for almost all investigated metal oxides, the dissolution in aqueous HCl is higher [133]. Comparing the quantitative solubilities of metal oxides in different reports, e.g., [133] with [135] and [138], a significant deviation becomes apparent. Certainly, a variation of the reaction temperature by 10 K will influence the solubility. However, quantitative solubility data should always carefully be examined regarding its accurateness, as the experimental procedure, sample preparation as well as measuring method are sensitive to errors.

In order to determine the effect of the acidity of DESs on the dissolution of metal oxides, Mu et al. investigated the various DESs consisting of different alcohols (ethylene glycol, 1,2-propanediol, glycerol and 1,4-butanediol) and various organic acids (malonic, succinic, citric, maleic acid, molar ratio 4:1) at 60 °C. The best performance was found for the most acidic DES ethylene glycol-maleic acid. Furthermore, the deprotonation of the acid upon dissolution of a metal oxide was shown. This DES is suitable to separate light rare earths (≤gadolinium, except cerium) from heavy ones. However, for two examples tested, Eu₂O₃ and La₂O₃, the solubility was slightly lower than in aqueous hydrochloric acid (3.27 M) [139].

A more acidic DES consisting of *p*-toluenesulfonic acid and choline chloride in varying molar ratios was found by Binnemans et al. They reported a higher solubility of all metal oxides than in previously investigated DESs except for PbO. MnO₂, Fe₂O₃, Fe₃O₄ and CuO dissolved better in the DES than in aqueous HCl of a similar pH value. Furthermore, different molar ratios of the DES components appear to influence the dissolution of the metal oxides in different ways, opening possibilities for the development of highly selective leaching processes. Interestingly, usually the most acidic IL does not show the best solubility for metal oxides [134].

Furthermore, DESs were applied to the recycling of authentic mixed metal oxide samples. Thus, Binnemans et al. performed studies on the leaching of neodymium, dysprosium, praseodymium and gadolinium from roasted NdFeB magnets by three different DESs. Choline chloride in mixtures with twice the amount of either urea or ethylene glycol only showed a poor dissolution of iron and

neodymium oxide. A significantly better performance was found for choline chloride-lactic acid (molar ratio 1:2), attributed to the presence of acidic protons. Furthermore, the coordinating abilities of lactate or choline are assumed to have a positive effect [152].

In order to recycle the cathode of lithium ion batteries, Ajayan et al. investigated the solubility of LiCoO_2 by using the DES choline chloride-ethylene glycol (molar ratio 1:2). A beginning extraction of cobalt was found at 80 °C, whereby the extraction efficiency significantly increased with higher reaction temperatures (investigated up to 220 °C) and longer reaction times, hence, being comparable to phosphoric and hydrochloric acid. Apparently, during dissolution, cobalt(III) is reduced to cobalt(II) which might involve the oxidation of ethylene glycol. However, an electrodeposition of cobalt allows the reuse of the DES in additional cycles. The leaching efficiency of lithium for LiCoO_2 exceeds the one of cobalt [153].

Using Brønsted-acidic DESs, improves the solubility of metal oxides. This is attributed to the same effects like in ILs; the water-forming reaction of the acidic protons with the oxygen atoms of the metal oxides has a dissolution-supporting effect. Subsequently, the carboxylate group can build up adequate interactions to the metal ion via coordination. However, only in a few cases, the solubility in a DES exceeds the one in mineral acids. In this regard, the investigation of DESs with a sulphuric acid functionalised component might be promising. But even the so far investigated DESs could be interesting as a replacement of mineral acids in order to avoid aqueous waste in conventional metal recovery processes.

3.2.3. Conclusion on Dissolution of Metal Oxides in DESs

In recent years, less research has been performed concerning the dissolution of metal oxides in DESs than in ILs. Similar to ILs, the availability of coordinating ligands appears to be important for the dissolution of metal oxides. Furthermore, the presence of acidic protons as oxygen acceptors supports dissolution. However, the dissolution ability does not always seem to correlate with the acidity of the DES. Hence, other, yet not identified factors are assumed to have an effect. Further work is necessary to reveal the dissolution mechanisms and dissolved species present in the recently investigated systems.

The varying dissolution ability of different DESs could be used for selectively dissolving metals from oxide mixtures. The lower synthetic effort and costs compared to ILs might prove advantageous for future applications. Even if the dissolution ability might not reach the same degree as ILs, DESs could be a valuable part of dissolution and extraction processes. By the replacement of aqueous solvents, large amounts of waste might potentially be avoidable, if DESs can efficiently be recycled.

4. Conclusions

In the past two decades, research on the utilisation of ILs and DESs in the synthesis of metal oxides clearly focused on the production of nanoparticles. Typically, these reactions can be performed in other media as well, however, certain morphologies and phases could be made accessible and improvements towards the conventional methods were found. Therefore, ionothermal, microwave- as well as ultrasound-assisted methods seem to be suitable. However, in many cases, the underlying mechanisms and the structure-directing role of the IL are not clear, yet. Thus, further investigations in new systems still rather rely on educated guesses instead of allowing predictions and synthesis planning underpinned by assured knowledge. Therefore, future research should focus on getting insight into the reactions taking place on molecular level in order to understand and use the full potential of ILs and DESs. Besides, the synthesis of Al_2O_3 at a temperature as low as 150 °C reported by Zheng et al. highlights ILs as a promising solvent for new low-temperature reaction pathways for metal oxides. Again, further research should identify the reaction mechanism in order to apply this approach on larger systems as well as other metal oxides.

The research on the dissolution of metal oxides identified several ILs and DESs suitable to dissolve different metal oxides to a variable extent. Ongoing research on new systems produced ILs that were increasingly able to dissolve not readily soluble metal oxides, whereas a strong correlation with their

acidity became apparent. Therefore, it seems possible that in the future, suitable ILs for the dissolution of every metal oxide will be found. The different dissolution ability appears to be a promising property for the selective leaching of metals from ores as well as waste. Despite DESs often showing no better solubility for metal oxides than conventional aqueous solvents, they should be considered as low-cost alternative to ILs, where possible. Especially for the selective leaching of metal oxides from waste, ILs as well as DESs might be used together in optimised processes. In future research, also downstream chemistry proceeding from such metal oxide solutions should gain centre stage. Thus, suitable methods for the synthesis of chemicals in demand as well as the electrodeposition of metals should be developed.

New syntheses of metal oxides as well as new metal oxide processing paths without calcination steps and other high-temperature reactions could mean great energy savings and would be a step towards a greener future. Completely new reaction pathways could have impact on industrial processes. However, because of the high costs of some ILs, it will be important to recycle and reuse them.

Altogether, the research field of metal oxide chemistry in ILs and DES still seems to be at its beginning. A lot of further research will be necessary in order to understand the processes taking place, apply them to desired systems and maybe even bring them to industrial relevance.

Author Contributions: Writing—original draft preparation, J.R.; writing—review and editing; supervision; project administration; funding acquisition, M.R. All authors have read and agreed to the published version of the manuscript.

Funding: This research was supported by the German Research Foundation (DFG) within the framework of the Priority Program SPP 1708.

Conflicts of Interest: The authors declare no conflict of interest.

References

1. Jolivet, J.-P.; Henry, M.; Livage, J. *Metal Oxide Chemistry and Synthesis: From Solution to Solid State*; Wiley: Chichester, UK, 2000; ISBN 978-0-471-97056-9.
2. Cao, H.; Xu, J.Y.; Zhang, D.Z.; Chang, S.-H.; Ho, S.T.; Seelig, E.W.; Liu, X.; Chang, R.P.H. Spatial Confinement of Laser Light in Active Random Media. *Phys. Rev. Lett.* **2000**, *84*, 5584–5587. [[CrossRef](#)] [[PubMed](#)]
3. Zhang, H.; Ma, X.; Xu, J.; Niu, J.; Yang, D. Arrays of ZnO nanowires fabricated by a simple chemical solution route. *Nanotechnology* **2003**, *14*, 423–426. [[CrossRef](#)]
4. Li, Z.; Xiong, Y.; Xie, Y. Selected-Control Synthesis of ZnO Nanowires and Nanorods via a PEG-Assisted Route. *Inorg. Chem.* **2003**, *42*, 8105–8109. [[CrossRef](#)] [[PubMed](#)]
5. Yan, H.; He, R.; Pham, J.; Yang, P. Morphogenesis of One-Dimensional ZnO Nano- and Microcrystals. *Adv. Mater.* **2003**, *15*, 402–405. [[CrossRef](#)]
6. Yang, P.; Zhao, D.; Margolese, D.I.; Chmelka, B.F.; Stucky, G.D. Block Copolymer Templating Syntheses of Mesoporous Metal Oxides with Large Ordering Lengths and Semicrystalline Framework. *Chem. Mater.* **1999**, *11*, 2813–2826. [[CrossRef](#)]
7. Sun, C.; Li, H.; Chen, L. Nanostructured ceria-based materials: Synthesis, properties, and applications. *Energy Environ. Sci.* **2012**, *5*, 8475. [[CrossRef](#)]
8. Sun, C.; Sun, J.; Xiao, G.; Zhang, H.; Qiu, X.; Li, H.; Chen, L. Mesoscale Organization of Nearly Monodisperse Flowerlike Ceria Microspheres. *J. Phys. Chem. B* **2006**, *110*, 13445–13452. [[CrossRef](#)]
9. Sun, C.; Chen, L. Controllable Synthesis of Shuttle-Shaped Ceria and Its Catalytic Properties for CO Oxidation. *Eur. J. Inorg. Chem.* **2009**, *2009*, 3883–3887. [[CrossRef](#)]
10. Araújo, V.D.; Avansi, W.; de Carvalho, H.B.; Moreira, M.L.; Longo, E.; Ribeiro, C.; Bernardi, M.I.B. CeO₂ nanoparticles synthesized by a microwave-assisted hydrothermal method: Evolution from nanospheres to nanorods. *CrystEngComm* **2012**, *14*, 1150–1154. [[CrossRef](#)]
11. Wang, Y.; Mori, T.; Li, J.-G.; Ikegami, T. Low-Temperature Synthesis of Praseodymium-Doped Ceria Nanopowders. *J. Am. Ceram. Soc.* **2004**, *85*, 3105–3107. [[CrossRef](#)]
12. Verma, A.; Karar, N.; Bakhshi, A.K.; Chander, H.; Shivaprasad, S.M.; Agnihotry, S.A. Structural, morphological and photoluminescence characteristics of sol-gel derived nano phase CeO₂ films deposited using citric acid. *J. Nanopart. Res.* **2007**, *9*, 317–322. [[CrossRef](#)]

13. Guillou, N.; Nistor, L.C.; Fuess, H.; Hahn, H. Microstructural studies of nanocrystalline CeO₂ produced by gas condensation. *Nanostruct. Mater.* **1997**, *8*, 545–557. [CrossRef]
14. U.S. Geological Survey Mineral Commodity Summaries. Available online: <https://s3-us-west-2.amazonaws.com/prd-wret/assets/palladium/production/mineral-pubs/mcs/mcs2018.pdf> (accessed on 3 September 2018).
15. Holleman, A.F.; Wiberg, E.; Wiberg, N.; Fischer, G. *Anorganische Chemie*; De Gruyter: Berlin, Germany; Boston, MA, USA, 2017; ISBN 978-3-11-049585-0.
16. Rabie, K.A. A group separation and purification of Sm, Eu and Gd from Egyptian beach monazite mineral using solvent extraction. *Hydrometallurgy* **2007**, *85*, 81–86. [CrossRef]
17. Um, N.; Hirato, T. Dissolution Behavior of La₂O₃, Pr₂O₃, Nd₂O₃, CaO and Al₂O₃ in Sulfuric Acid Solutions and Study of Cerium Recovery from Rare Earth Polishing Powder Waste via Two-Stage Sulfuric Acid Leaching. *Mater. Trans.* **2013**, *54*, 713–719. [CrossRef]
18. Jayachandran, K.; Gupta, R.; Chandrakumar, K.R.S.; Goswami, D.; Noronha, D.M.; Paul, S.; Kannan, S. Remarkably enhanced direct dissolution of plutonium oxide in task-specific ionic liquid: Insights from electrochemical and theoretical investigations. *Chem. Commun.* **2019**, *55*, 1474–1477. [CrossRef] [PubMed]
19. *Ionic Liquids in Synthesis*; Wasserscheid, P. (Ed.) Wiley-VCH: Weinheim, Germany, 2002; ISBN 978-3-527-31239-9.
20. Smith, E.L.; Abbott, A.P.; Ryder, K.S. Deep Eutectic Solvents (DESs) and Their Applications. *Chem. Rev.* **2014**, *114*, 11060–11082. [CrossRef]
21. Pechtl, M.H.G.; Campbell, P.S. Metal oxide and bimetallic nanoparticles in ionic liquids: Synthesis and application in multiphase catalysis. *Nanotechnol. Rev.* **2013**, *2*. [CrossRef]
22. Abbott, A.P.; Frisch, G.; Hartley, J.; Ryder, K.S. Processing of metals and metal oxides using ionic liquids. *Green Chem.* **2011**, *13*, 471. [CrossRef]
23. Abbott, A.P.; Frisch, G.; Ryder, K.S. Metal complexation in ionic liquids. *Annu. Rep. Prog. Chem. Sect. A Inorg. Chem.* **2008**, *104*, 21. [CrossRef]
24. Mele, A.; Tran, C.D.; De Paoli Lacerda, S.H. The Structure of a Room-Temperature Ionic Liquid with and without Trace Amounts of Water: The Role of C–H···O and C–H···F Interactions in 1-n-Butyl-3-Methylimidazolium Tetrafluoroborate. *Angew. Chem. Int. Ed.* **2003**, *42*, 4364–4366. [CrossRef]
25. Liu, X.; Duan, X.; Qin, Q.; Wang, Q.; Zheng, W. Ionic liquid-assisted solvothermal synthesis of oriented self-assembled Fe₃O₄ nanoparticles into monodisperse nanoflakes. *CrystEngComm* **2013**, *15*, 3284. [CrossRef]
26. Morris, R.E. Ionothermal synthesis-ionic liquids as functional solvents in the preparation of crystalline materials. *Chem. Commun.* **2009**, 2990–2998. [CrossRef] [PubMed]
27. Alammar, T.; Slowing, I.I.; Andereg, J.; Mudring, A.-V. Ionic-Liquid-Assisted Microwave Synthesis of Solid Solutions of Sr_{1-x}Ba_xSnO₃ Perovskite for Photocatalytic Applications. *ChemSusChem* **2017**, *10*, 3387–3401. [CrossRef] [PubMed]
28. Alammar, T.; Mudring, A.-V. Facile ultrasound-assisted synthesis of ZnO nanorods in an ionic liquid. *Mater. Lett.* **2009**, *63*, 732–735. [CrossRef]
29. Alammar, T.; Birkner, A.; Mudring, A.-V. Ultrasound-Assisted Synthesis of CuO Nanorods in a Neat Room-Temperature Ionic Liquid. *Eur. J. Inorg. Chem.* **2009**, *2009*, 2765–2768. [CrossRef]
30. Alammar, T.; Noei, H.; Wang, Y.; Grünert, W.; Mudring, A.-V. Ionic Liquid-Assisted Sonochemical Preparation of CeO₂ Nanoparticles for CO Oxidation. *ACS Sustain. Chem. Eng.* **2015**, *3*, 42–54. [CrossRef]
31. Alammar, T.; Birkner, A.; Shekhah, O.; Mudring, A.-V. Sonochemical preparation of TiO₂ nanoparticles in the ionic liquid 1-(3-hydroxypropyl)-3-methylimidazolium-bis(trifluoromethylsulfonyl)amide. *Mater. Chem. Phys.* **2010**, *120*, 109–113. [CrossRef]
32. Louisnard, O.; González-García, J. Acoustic Cavitation. In *Ultrasound Technologies for Food and Bioprocessing*; Feng, H., Barbosa-Canovas, G., Weiss, J., Eds.; Springer: New York, NY, USA, 2011; pp. 13–64. ISBN 978-1-4419-7471-6.
33. Merouani, S.; Hamdaoui, O.; Haddad, B. Acoustic cavitation in 1-butyl-3-methylimidazolium bis(trifluoromethyl-sulfonyl)imide based ionic liquid. *Ultrason. Sonochem.* **2018**, *41*, 143–155. [CrossRef]
34. Voepel, P.; Smarsly, B.M. Synthesis of Titanium Oxide Nanostructures in Ionic Liquids. *Z. Anorg. Allg. Chem.* **2017**, *643*, 3–13. [CrossRef]
35. Zhang, H.; Banfield, J.F. Understanding Polymorphic Phase Transformation Behavior during Growth of Nanocrystalline Aggregates: Insights from TiO₂. *J. Phy. Chem. B* **2000**, *104*, 3481–3487. [CrossRef]
36. Patnaik, P. *Handbook of Inorganic Chemicals*; McGraw-Hill: New York, NY, USA, 2003; ISBN 978-0-07-049439-8.

37. Kaper, H.; Endres, F.; Djerdj, I.; Antonietti, M.; Smarsly, B.M.; Maier, J.; Hu, Y.-S. Direct Low-Temperature Synthesis of Rutile Nanostructures in Ionic Liquids. *Small* **2007**, *3*, 1753–1763. [[CrossRef](#)] [[PubMed](#)]
38. Zhou, Y.; Antonietti, M. Synthesis of Very Small TiO₂ Nanocrystals in a Room-Temperature Ionic Liquid and Their Self-Assembly toward Mesoporous Spherical Aggregates. *J. Am. Chem. Soc.* **2003**, *125*, 14960–14961. [[CrossRef](#)] [[PubMed](#)]
39. Ding, K.; Miao, Z.; Liu, Z.; Zhang, Z.; Han, B.; An, G.; Miao, S.; Xie, Y. Facile Synthesis of High Quality TiO₂ Nanocrystals in Ionic Liquid via a Microwave-Assisted Process. *J. Am. Chem. Soc.* **2007**, *129*, 6362–6363. [[CrossRef](#)] [[PubMed](#)]
40. Alammar, T.; Noei, H.; Wang, Y.; Mudring, A.-V. Mild yet phase-selective preparation of TiO₂ nanoparticles from ionic liquids—A critical study. *Nanoscale* **2013**, *5*, 8045. [[CrossRef](#)]
41. Nakashima, T.; Kimizuka, N. Interfacial Synthesis of Hollow TiO₂ Microspheres in Ionic Liquids. *J. Am. Chem. Soc.* **2003**, *125*, 6386–6387. [[CrossRef](#)]
42. Dylla, A.G.; Henkelman, G.; Stevenson, K.J. Lithium Insertion in Nanostructured TiO₂(B) Architectures. *Acc. Chem. Res.* **2013**, *46*, 1104–1112. [[CrossRef](#)]
43. Dylla, A.G.; Stevenson, K.J. Electrochemical and Raman spectroscopy identification of morphological and phase transformations in nanostructured TiO₂(B). *J. Mater. Chem. A* **2014**, *2*, 20331–20337. [[CrossRef](#)]
44. Etacheri, V.; Yourey, J.E.; Bartlett, B.M. Chemically Bonded TiO₂-Bronze Nanosheet/Reduced Graphene Oxide Hybrid for High-Power Lithium Ion Batteries. *ACS Nano* **2014**, *8*, 1491–1499. [[CrossRef](#)]
45. Yin, S.; Wu, J.; Aki, M.; Sato, T. Photocatalytic hydrogen evolution with fibrous titania prepared by the solvothermal reactions of protonic layered tetratitanate (H₂Ti₄O₉). *Int. J. Inorg. Mater.* **2000**, *2*, 325–331. [[CrossRef](#)]
46. Yang, D.; Liu, H.; Zheng, Z.; Yuan, Y.; Zhao, J.; Waclawik, E.R.; Ke, X.; Zhu, H. An Efficient Photocatalyst Structure: TiO₂(B) Nanofibers with a Shell of Anatase Nanocrystals. *J. Am. Chem. Soc.* **2009**, *131*, 17885–17893. [[CrossRef](#)]
47. Kaper, H.; Sallard, S.; Djerdj, I.; Antonietti, M.; Smarsly, B.M. Toward a Low-Temperature Sol-Gel Synthesis of TiO₂(B) Using Mixtures of Surfactants and Ionic Liquids. *Chem. Mater.* **2010**, *22*, 3502–3510. [[CrossRef](#)]
48. Voepel, P.; Seitz, C.; Waack, J.M.; Zahn, S.; Leichtweiß, T.; Zaichenko, A.; Mollenhauer, D.; Amenitsch, H.; Voggenreiter, M.; Polarz, S.; et al. Peering into the Mechanism of Low-Temperature Synthesis of Bronze-type TiO₂ in Ionic Liquids. *Cryst. Growth Des.* **2017**, *17*, 5586–5601. [[CrossRef](#)]
49. Wessel, C.; Zhao, L.; Urban, S.; Ostermann, R.; Djerdj, I.; Smarsly, B.M.; Chen, L.; Hu, Y.-S.; Sallard, S. Ionic-Liquid Synthesis Route of TiO₂(B) Nanoparticles for Functionalized Materials. *Chem. Eur. J.* **2011**, *17*, 775–779. [[CrossRef](#)] [[PubMed](#)]
50. Mansfeldova, V.; Laskova, B.; Krysova, H.; Zukalova, M.; Kavan, L. Synthesis of nanostructured TiO₂ (anatase) and TiO₂(B) in ionic liquids. *Catal. Today* **2014**, *230*, 85–90. [[CrossRef](#)]
51. Li, Z.; Geßner, A.; Richters, J.-P.; Kalden, J.; Voss, T.; Kübel, C.; Taubert, A. Hollow Zinc Oxide Mesocrystals from an Ionic Liquid Precursor (ILP). *Adv. Mater.* **2008**, *20*, 1279–1285. [[CrossRef](#)]
52. Li, Z.; Shkilnyy, A.; Taubert, A. Room Temperature ZnO Mesocrystal Formation in the Hydrated Ionic Liquid Precursor (ILP) Tetrabutylammonium Hydroxide. *Cryst. Growth Des.* **2008**, *8*, 4526–4532. [[CrossRef](#)]
53. Taubert, A.; Kübel, C.; Martin, D.C. Polymer-Induced Microstructure Variation in Zinc Oxide Crystals Precipitated from Aqueous Solution. *J. Phys. Chem. B* **2003**, *107*, 2660–2666. [[CrossRef](#)]
54. Taubert, A.; Glasser, G.; Palms, D. Kinetics and Particle Formation Mechanism of Zinc Oxide Particles in Polymer-Controlled Precipitation from Aqueous Solution. *Langmuir* **2002**, *18*, 4488–4494. [[CrossRef](#)]
55. Taubert, A.; Palms, D.; Weiss, Ö.; Piccini, M.-T.; Batchelder, D.N. Polymer-Assisted Control of Particle Morphology and Particle Size of Zinc Oxide Precipitated from Aqueous Solution. *Chem. Mater.* **2002**, *14*, 2594–2601. [[CrossRef](#)]
56. Edwards, D.A.; Hayward, R.N. Transition metal acetates. *Can. J. Chem.* **1968**, *46*, 3443–3446. [[CrossRef](#)]
57. Wang, L.; Chang, L.; Zhao, B.; Yuan, Z.; Shao, G.; Zheng, W. Systematic Investigation on Morphologies, Forming Mechanism, Photocatalytic and Photoluminescent Properties of ZnO Nanostructures Constructed in Ionic Liquids. *Inorg. Chem.* **2008**, *47*, 1443–1452. [[CrossRef](#)] [[PubMed](#)]
58. Ye, X.R.; Jia, D.Z.; Yu, J.Q.; Xin, X.Q.; Xue, Z.L. One-Step Solid-State Reactions at Ambient Temperatures—A Novel Approach to Nanocrystal Synthesis. *Adv. Mater.* **1999**, *11*, 941–942. [[CrossRef](#)]
59. Zhu, H.; Huang, J.-F.; Pan, Z.; Dai, S. Ionothermal Synthesis of Hierarchical ZnO Nanostructures from Ionic-Liquid Precursors. *Chem. Mater.* **2006**, *18*, 4473–4477. [[CrossRef](#)]

60. Taubert, A.; Uhlmann, A.; Hedderich, A.; Kirchoff, K. CuO Particles from Ionic Liquid/Water Mixtures: Evidence for Growth via Cu(OH)₂ Nanorod Assembly and Fusion. *Inorg. Chem.* **2008**, *47*, 10758–10764. [[CrossRef](#)]
61. Li, Z.; Rabu, P.; Strauch, P.; Manton, A.; Taubert, A. Uniform Metal (Hydr)Oxide Particles from Water/Ionic Liquid Precursor (ILP) Mixtures. *Chem. Eur. J.* **2008**, *14*, 8409–8417. [[CrossRef](#)]
62. Ma, J.; Wang, T.; Duan, X.; Lian, J.; Liu, Z.; Zheng, W. Ionothermal synthesis of aggregated α -Fe₂O₃ nanoplates and their magnetic properties. *Nanoscale* **2011**, *3*, 4372. [[CrossRef](#)]
63. Wang, Y.; Maksimuk, S.; Shen, R.; Yang, H. Synthesis of iron oxide nanoparticles using a freshly-made or recycled imidazolium-based ionic liquid. *Green Chem.* **2007**, *9*, 1051. [[CrossRef](#)]
64. Jacob, D.S.; Bitton, L.; Grinblat, J.; Felner, I.; Koltypin, Y.; Gedanken, A. Are Ionic Liquids Really a Boon for the Synthesis of Inorganic Materials? A General Method for the Fabrication of Nanosized Metal Fluorides. *Chem. Mater.* **2006**, *18*, 3162–3168. [[CrossRef](#)]
65. Van Dao, D.; Nguyen, T.T.D.; Majhi, S.M.; Adilbish, G.; Lee, H.-J.; Yu, Y.-T.; Lee, I.-H. Ionic liquid-supported synthesis of CeO₂ nanoparticles and its enhanced ethanol gas sensing properties. *Mater. Chem. Phys.* **2019**, *231*, 1–8. [[CrossRef](#)]
66. Li, Z.-X.; Li, L.-L.; Yuan, Q.; Feng, W.; Xu, J.; Sun, L.-D.; Song, W.-G.; Yan, C.-H. Sustainable and Facile Route to Nearly Monodisperse Spherical Aggregates of CeO₂ Nanocrystals with Ionic Liquids and Their Catalytic Activities for CO Oxidation. *J. Phys. Chem. C* **2008**, *112*, 18405–18411. [[CrossRef](#)]
67. Alammari, T.; Chow, Y.-K.; Mudring, A.-V. Energy efficient microwave synthesis of mesoporous Ce_{0.5}M_{0.5}O₂ (Ti, Zr, Hf) nanoparticles for low temperature CO oxidation in an ionic liquid—A comparative study. *New J. Chem.* **2015**, *39*, 1339–1347. [[CrossRef](#)]
68. Lian, J.; Ma, J.; Duan, X.; Kim, T.; Li, H.; Zheng, W. One-step ionothermal synthesis of γ -Al₂O₃ mesoporous nanoflakes at low temperature. *Chem. Commun.* **2010**, *46*, 2650. [[CrossRef](#)] [[PubMed](#)]
69. Bonne, M.; Gaudin, P.; Gu, Y.; Jérôme, F.; Pouilloux, Y.; Duprez, D.; Royer, S. Ionic Liquids Mediated Ionothermal Process for the One-Step Synthesis of High Surface Area Alumina Supported Noble Metals. *Mod. Res. Catal.* **2013**, *02*, 28–35. [[CrossRef](#)]
70. Kinoshita, K.; Minami, H.; Tarutani, Y.; Tajima, K.; Okubo, M.; Yanagimoto, H. Preparations of Polystyrene/Aluminum Hydroxide and Polystyrene/Alumina Composite Particles in an Ionic Liquid. *Langmuir* **2011**, *27*, 4474–4480. [[CrossRef](#)] [[PubMed](#)]
71. Ji, X.; Tang, S.; Gu, L.; Liu, T.; Zhang, X. Synthesis of rod-like mesoporous γ -Al₂O₃ by an ionic liquid-assisted sol-gel method. *Mater. Lett.* **2015**, *151*, 20–23. [[CrossRef](#)]
72. Park, H.; Yang, S.H.; Jun, Y.S.; Hong, W.H.; Kang, J.K. Facile Route to Synthesize Large-Mesoporous γ -Alumina by Room Temperature Ionic Liquids. *Chem. Mater.* **2007**, *19*, 535–542. [[CrossRef](#)]
73. Li Juan, C.; Sheng Mao, Z.; Zhi Shen, W.; Zhi Jun, Z.; Hong Xin, D. Preparation of PbS-type PbO nanocrystals in a room-temperature ionic liquid. *Mater. Lett.* **2005**, *59*, 3119–3121. [[CrossRef](#)]
74. Bühler, G.; Thölmann, D.; Feldmann, C. One-Pot Synthesis of Highly Conductive Indium Tin Oxide Nanocrystals. *Adv. Mater.* **2007**, *19*, 2224–2227. [[CrossRef](#)]
75. Zhang, T.; Doert, T.; Ruck, M. Solvothermal synthesis and enhanced photo-electrochemical performance of hierarchically structured strontium titanate micro-particles. *Dalton Trans.* **2017**, *46*, 14219–14225. [[CrossRef](#)]
76. Abbott, A.P.; Capper, G.; Davies, D.L.; Munro, H.L.; Rasheed, R.K.; Tambyrajah, V. Preparation of novel, moisture-stable, Lewis-acidic ionic liquids containing quaternary ammonium salts with functional side chains. *Chem. Commun.* **2001**, 2010–2011. [[CrossRef](#)]
77. Abbott, A.P.; Capper, G.; Davies, D.L.; Rasheed, R.K.; Tambyrajah, V. Novel solvent properties of choline chloride/urea mixtures. *Chem. Commun.* **2003**, 70–71. [[CrossRef](#)] [[PubMed](#)]
78. Chen, F.; Xie, S.; Zhang, J.; Liu, R. Synthesis of spherical Fe₃O₄ magnetic nanoparticles by co-precipitation in choline chloride/urea deep eutectic solvent. *Mater. Lett.* **2013**, *112*, 177–179. [[CrossRef](#)]
79. Gu, C.D.; Huang, M.L.; Ge, X.; Zheng, H.; Wang, X.L.; Tu, J.P. NiO electrode for methanol electro-oxidation: Mesoporous vs. nanoparticulate. *Int. J. Hydrogen Energy* **2014**, *39*, 10892–10901. [[CrossRef](#)]
80. Gu, C.; Zhang, H.; Wang, X.; Tu, J. One-pot synthesis of SnO₂/reduced graphene oxide nanocomposite in ionic liquid-based solution and its application for lithium ion batteries. *Mater. Res. Bull.* **2013**, *48*, 4112–4117. [[CrossRef](#)]

81. Ge, X.; Gu, C.D.; Lu, Y.; Wang, X.L.; Tu, J.P. A versatile protocol for the ionothermal synthesis of nanostructured nickel compounds as energy storage materials from a choline chloride-based ionic liquid. *J. Mater. Chem. A* **2013**, *1*, 13454–13461. [[CrossRef](#)]
82. Ge, X.; Gu, C.D.; Wang, X.L.; Tu, J.P. Correlation between Microstructure and Electrochemical Behavior of the Mesoporous Co₃O₄ Sheet and Its Ionothermal Synthesized Hydrotalcite-like α -Co(OH)₂ Precursor. *J. Phys. Chem. C* **2014**, *118*, 911–923. [[CrossRef](#)]
83. Zhou, X.; Xie, Z.-X.; Jiang, Z.-Y.; Kuang, Q.; Zhang, S.-H.; Xu, T.; Huang, R.-B.; Zheng, L.-S. Formation of ZnO hexagonal micro-pyramids: A successful control of the exposed polar surfaces with the assistance of an ionic liquid. *Chem. Commun.* **2005**, 5572–5574. [[CrossRef](#)]
84. Xiong, Q.Q.; Tu, J.P.; Ge, X.; Wang, X.L.; Gu, C.D. One-step synthesis of hematite nanospindles from choline chloride/urea deep eutectic solvent with highly powerful storage versus lithium. *J. Power Sources* **2015**, *274*, 1–7. [[CrossRef](#)]
85. Hammond, O.S.; Eslava, S.; Smith, A.J.; Zhang, J.; Edler, K.J. Microwave-assisted deep eutectic-solvent thermal preparation of iron oxide nanoparticles for photoelectrochemical solar water splitting. *J. Mater. Chem. A* **2017**, *5*, 16189–16199. [[CrossRef](#)]
86. Zheng, H.; Gu, C.-D.; Wang, X.-L.; Tu, J.-P. Fast synthesis and optical property of SnO nanoparticles from choline chloride-based ionic liquid. *J. Nanopart. Res.* **2014**, *16*, 2288. [[CrossRef](#)]
87. Li, F.; Song, J.; Yang, H.; Gan, S.; Zhang, Q.; Han, D.; Ivaska, A.; Niu, L. One-step synthesis of graphene/SnO₂ nanocomposites and its application in electrochemical supercapacitors. *Nanotechnology* **2009**, *20*, 455602. [[CrossRef](#)] [[PubMed](#)]
88. Gu, C.D.; Mai, Y.J.; Zhou, J.P.; Tu, J.P. SnO₂ nanocrystallite: Novel synthetic route from deep eutectic solvent and lithium storage performance. *Funct. Mater. Lett.* **2011**, *04*, 377–381. [[CrossRef](#)]
89. Oderinde, O.; Kang, M.; Kalulu, M.; Yao, F.; Fu, G. Facile synthesis and study of the photochromic properties of deep eutectic solvent-templated cuboctahedral-WO₃/MoO₃ nanocomposites. *Superlattices Microstruct.* **2019**, *125*, 103–112. [[CrossRef](#)]
90. Minami, H.; Kinoshita, K.; Tsuji, T.; Yanagimoto, H. Preparation of Highly Crystalline Magnesium Oxide and Polystyrene/Magnesium Hydroxide Composite Particles by Sol-gel Processes in an Ionic Liquid. *J. Phys. Chem. C* **2012**, *116*, 14568–14574. [[CrossRef](#)]
91. Alammar, T.; Hamm, I.; Grasmik, V.; Wark, M.; Mudring, A.-V. Microwave-Assisted Synthesis of Perovskite SrSnO₃ Nanocrystals in Ionic Liquids for Photocatalytic Applications. *Inorg. Chem.* **2017**, *56*, 6920–6932. [[CrossRef](#)]
92. Wang, C.; Yang, Y.; Chen, Z.; He, C.; Su, J.; Wen, Y. A mild process for the synthesis of Na₂Ti₃O₇ as an anode material for sodium-ion batteries in deep eutectic solvent. *J. Mater. Sci. Mater. Electron.* **2019**, *30*, 8422–8427. [[CrossRef](#)]
93. Thorat, G.M.; Jadhav, H.S.; Roy, A.; Chung, W.-J.; Seo, J.G. Dual Role of Deep Eutectic Solvent as a Solvent and Template for the Synthesis of Octahedral Cobalt Vanadate for an Oxygen Evolution Reaction. *ACS Sustain. Chem. Eng.* **2018**, *6*, 16255–16266. [[CrossRef](#)]
94. Boston, R.; Foeller, P.Y.; Sinclair, D.C.; Reaney, I.M. Synthesis of Barium Titanate Using Deep Eutectic Solvents. *Inorg. Chem.* **2017**, *56*, 542–547. [[CrossRef](#)]
95. Lu, W.; Yuan, P.; Wei, F.; Li, W.; Zhou, Y.; Zheng, W.; Zhang, G. Porous Ir-Sn Binary Oxide Nanorod Assembly as an Efficient Electrocatalyst for Water Oxidation. *Int. J. Electrochem. Sci.* **2018**, *13*, 3235–3245. [[CrossRef](#)]
96. Söldner, A.; Zach, J.; Iwanow, M.; Gärtner, T.; Schlosser, M.; Pfitzner, A.; König, B. Preparation of Magnesium, Cobalt and Nickel Ferrite Nanoparticles from Metal Oxides using Deep Eutectic Solvents. *Chem. Eur. J.* **2016**, *22*, 13108–13113. [[CrossRef](#)]
97. Mohapatra, P.K.; Kandwal, P.; Iqbal, M.; Huskens, J.; Murali, M.S.; Verboom, W. A novel CMPO-functionalized task specific ionic liquid: Synthesis, extraction and spectroscopic investigations of actinide and lanthanide complexes. *Dalton Trans.* **2013**, *42*, 4343. [[CrossRef](#)] [[PubMed](#)]
98. Boyd, R.; Jin, L.; Nockemann, P.; Robertson, P.K.J.; Stella, L.; Ruhela, R.; Seddon, K.R.; Gunaratne, H.Q.N. Ionic liquids tethered to a preorganised 1,2-diamide motif for extraction of lanthanides. *Green Chem.* **2019**, *21*, 2583–2588. [[CrossRef](#)]
99. Mehdi, H.; Binnemans, K.; Van Hecke, K.; Van Meervelt, L.; Nockemann, P. Hydrophobic ionic liquids with strongly coordinating anions. *Chem. Commun.* **2010**, *46*, 234–236. [[CrossRef](#)] [[PubMed](#)]

100. Dietz, M.L. Ionic Liquids as Extraction Solvents: Where do We Stand? *Sep. Sci. Technol.* **2006**, *41*, 2047–2063. [[CrossRef](#)]
101. Wellens, S.; Brooks, N.R.; Thijs, B.; Meervelt, L.V.; Binnemans, K. Carbene formation upon reactive dissolution of metal oxides in imidazolium ionic liquids. *Dalton Trans.* **2014**, *43*, 3443–3452. [[CrossRef](#)]
102. Nockemann, P.; Thijs, B.; Pittois, S.; Thoen, J.; Glorieux, C.; Van Hecke, K.; Van Meervelt, L.; Kirchner, B.; Binnemans, K. Task-Specific Ionic Liquid for Solubilizing Metal Oxides. *J. Phys. Chem. B* **2006**, *110*, 20978–20992. [[CrossRef](#)]
103. Nockemann, P.; Thijs, B.; Hecke, K.V.; Meervelt, L.V.; Binnemans, K. Polynuclear Metal Complexes Obtained from the Task-Specific Ionic Liquid Betainium Bistriflimide. *Cryst. Growth Des.* **2008**, *8*, 1353–1363. [[CrossRef](#)]
104. Nockemann, P.; Thijs, B.; Parac-Vogt, T.N.; Van Hecke, K.; Van Meervelt, L.; Tinant, B.; Hartenbach, I.; Schleid, T.; Ngan, V.T.; Nguyen, M.T.; et al. Carboxyl-Functionalized Task-Specific Ionic Liquids for Solubilizing Metal Oxides. *Inorg. Chem.* **2008**, *47*, 9987–9999. [[CrossRef](#)]
105. Dupont, D.; Raiguel, S.; Binnemans, K. Sulfonic acid functionalized ionic liquids for dissolution of metal oxides and solvent extraction of metal ions. *Chem. Commun.* **2015**, *51*, 9006–9009. [[CrossRef](#)]
106. Richter, J.; Ruck, M. Dissolution of metal oxides in task-specific ionic liquid. *RSC Adv.* **2019**, *9*, 29699–29710. [[CrossRef](#)]
107. Mahjoor, P.; Lattur, S.E. Synthesis and Structural Characterization of [bpyr]₄[V₄O₄Cl₁₂] and [bpyr]₄[Bi₄Cl₁₆] grown in Ionic Liquid [bpyr][AlCl₄] (bpyr = 1-Butylpyridinium). *Cryst. Growth Des.* **2009**, *9*, 1385–1389. [[CrossRef](#)]
108. Wellens, S.; Vander Hoogerstraete, T.; Möller, C.; Thijs, B.; Luyten, J.; Binnemans, K. Dissolution of metal oxides in an acid-saturated ionic liquid solution and investigation of the back-extraction behaviour to the aqueous phase. *Hydrometallurgy* **2014**, *144–145*, 27–33. [[CrossRef](#)]
109. Dupont, D.; Renders, E.; Binnemans, K. Alkylsulfuric acid ionic liquids: A promising class of strongly acidic room-temperature ionic liquids. *Chem. Commun.* **2016**, *52*, 4640–4643. [[CrossRef](#)] [[PubMed](#)]
110. Dupont, D.; Renders, E.; Raiguel, S.; Binnemans, K. New metal extractants and super-acidic ionic liquids derived from sulfamic acid. *Chem. Commun.* **2016**, *52*, 7032–7035. [[CrossRef](#)] [[PubMed](#)]
111. Billard, I.; Gaillard, C.; Hennig, C. Dissolution of UO₂, UO₃ and of some lanthanide oxides in BumimTf₂N: Effect of acid and water and formation of UO₂(NO₃)³⁻. *Dalton Trans.* **2007**, 4214–4221. [[CrossRef](#)]
112. Zhang, B.; Yao, Y.; Shi, Z.; Xu, J.; Wang, Z. Direct Electrochemical Deposition of Lithium from Lithium Oxide in a Highly Stable Aluminium-Containing Solvate Ionic Liquid. *ChemElectroChem* **2018**, *5*, 3368–3372. [[CrossRef](#)]
113. Yeh, H.-W.; Tang, Y.-H.; Chen, P.-Y. Electrochemical study and extraction of Pb metal from Pb oxides and Pb sulfate using hydrophobic Brønsted acidic amide-type ionic liquid: A feasibility demonstration. *J. Electrochem. Soc.* **2018**, *811*, 68–77. [[CrossRef](#)]
114. Nockemann, P.; Thijs, B.; Lunstroot, K.; Parac-Vogt, T.N.; Görrler-Walrand, C.; Binnemans, K.; Van Hecke, K.; Van Meervelt, L.; Nikitenko, S.; Daniels, J.; et al. Speciation of Rare-Earth Metal Complexes in Ionic Liquids: A Multiple-Technique Approach. *Chem. Eur. J.* **2009**, *15*, 1449–1461. [[CrossRef](#)]
115. Yao, A.; Chu, T. Fe-containing ionic liquids as effective and recoverable oxidants for dissolution of UO₂ in the presence of imidazolium chlorides. *Dalton Trans.* **2013**, *42*, 8413. [[CrossRef](#)]
116. Zarzana, C.A.; Groenewold, G.S.; Benson, M.T.; Delmore, J.E.; Tsuda, T.; Hagiwara, R. Production of Gas-Phase Uranium Fluoroanions Via Solubilization of Uranium Oxides in the [1-Ethyl-3-Methylimidazolium]⁺[F(HF)_{2.3}] Ionic Liquid. *J. Am. Soc. Mass Spectrom.* **2018**, *29*, 1963–1970. [[CrossRef](#)]
117. Rao, C.J.; Venkatesan, K.A.; Nagarajan, K.; Srinivasan, T.G. Dissolution of uranium oxides and electrochemical behavior of U(VI) in task specific ionic liquid. *Radiochim. Acta* **2008**, *96*. [[CrossRef](#)]
118. Dai, S.; Shin, Y.S.; Toth, L.M.; Barnes, C.E. Comparative UV–Vis Studies of Uranyl Chloride Complex in Two Basic Ambient-Temperature Melt Systems: The Observation of Spectral and Thermodynamic Variations Induced via Hydrogen Bonding. *Inorg. Chem.* **1997**, *36*, 4900–4902. [[CrossRef](#)] [[PubMed](#)]
119. Wanigasekara, E.; Freiderich, J.W.; Sun, X.-G.; Meisner, R.A.; Luo, H.; Delmau, L.H.; Dai, S.; Moyer, B.A. Tandem dissolution of UO₃ in amide-based acidic ionic liquid and in situ electrodeposition of UO₂ with regeneration of the ionic liquid: A closed cycle. *Dalton Trans.* **2016**, *45*, 10151–10154. [[CrossRef](#)] [[PubMed](#)]
120. Nockemann, P.; Van Deun, R.; Thijs, B.; Huys, D.; Vanecht, E.; Van Hecke, K.; Van Meervelt, L.; Binnemans, K. Uranyl Complexes of Carboxyl-Functionalized Ionic Liquids. *Inorg. Chem.* **2010**, *49*, 3351–3360. [[CrossRef](#)] [[PubMed](#)]

121. Bell, R.C.; Castleman, A.W.; Thorn, D.L. Vanadium Oxide Complexes in Room-Temperature Chloroaluminate Molten Salts. *Inorg. Chem.* **1999**, *38*, 5709–5715. [[CrossRef](#)]
122. Liu, Z.; El Abedin, S.Z.; Endres, F. Dissolution of zinc oxide in a protic ionic liquid with the 1-methylimidazolium cation and electrodeposition of zinc from ZnO/ionic liquid and ZnO/ionic liquid–water mixtures. *Electrochem. Commun.* **2015**, *58*, 46–50. [[CrossRef](#)]
123. Chaumont, A.; Wipff, G. Solvation of Uranyl(II), Europium(III) and Europium(II) Cations in “Basic” Room-Temperature Ionic Liquids: A Theoretical Study. *Chem. Eur. J.* **2004**, *10*, 3919–3930. [[CrossRef](#)]
124. Dupont, D.; Binnemans, K. Recycling of rare earths from NdFeB magnets using a combined leaching/extraction system based on the acidity and thermomorphism of the ionic liquid [Hbet][Tf₂N]. *Green Chem.* **2015**, *17*, 2150–2163. [[CrossRef](#)]
125. Fan, F.-L.; Qin, Z.; Cao, S.-W.; Tan, C.-M.; Huang, Q.-G.; Chen, D.-S.; Wang, J.-R.; Yin, X.-J.; Xu, C.; Feng, X.-G. Highly Efficient and Selective Dissolution Separation of Fission Products by an Ionic Liquid [Hbet][Tf₂N]: A New Approach to Spent Nuclear Fuel Recycling. *Inorg. Chem.* **2019**, *58*, 603–609. [[CrossRef](#)]
126. Davris, P.; Marinos, D.; Balomenos, E.; Alexandri, A.; Gregou, M.; Pnias, D.; Paspaliaris, I. Leaching of rare earth elements from ‘Rödberg’ ore of Fe carbonate complex deposit, using the ionic liquid HbetTf₂N. *Hydrometallurgy* **2018**, *175*, 20–27. [[CrossRef](#)]
127. Davris, P.; Balomenos, E.; Pnias, D.; Paspaliaris, I. Developing New Process for Selective Extraction of Rare Earth Elements from Bauxite Residue Based on Functionalized Ionic Liquids. In *Light Metals 2018*; Martin, O., Ed.; Springer International Publishing: Cham, Switzerland, 2018; pp. 149–156. ISBN 978-3-319-72283-2.
128. Li, H.; Shao, H.; Wang, Y.; Qin, D.; Liu, B.; Zhang, W.; Yan, W. Soft material with intense photoluminescence obtained by dissolving Eu₂O₃ and organic ligand into a task-specific ionic liquid. *Chem. Commun.* **2008**, 5209–5211. [[CrossRef](#)] [[PubMed](#)]
129. Mawire, G.; van Dyk, L. Extraction of Scandium (Sc) Using a Task-Specific Ionic Liquid Protonated Betaine Bis(Trifluoromethylsulfonyl)Imide [Hbet][Tf₂N]. In *Extraction 2018*; Davis, B.R., Moats, M.S., Wang, S., Gregurek, D., Kapusta, J., Battle, T.P., Schlesinger, M.E., Alvear Flores, G.R., Jak, E., Goodall, G., et al., Eds.; Springer International Publishing: Cham, Switzerland, 2018; pp. 2723–2734. ISBN 978-3-319-95021-1.
130. Schaeffer, N.; Grimes, S.; Cheeseman, C. Interactions between trivalent rare earth oxides and mixed [Hbet][Tf₂N]:H₂O systems in the development of a one-step process for the separation of light from heavy rare earth elements. *Inorg. Chim. Acta* **2016**, *439*, 55–60. [[CrossRef](#)]
131. Dupont, D.; Binnemans, K. Rare-earth recycling using a functionalized ionic liquid for the selective dissolution and revalorization of Y₂O₃:Eu³⁺ from lamp phosphor waste. *Green Chem.* **2015**, *17*, 856–868. [[CrossRef](#)]
132. Orefice, M.; Binnemans, K.; Vander Hoogerstraete, T. Metal coordination in the high-temperature leaching of roasted NdFeB magnets with the ionic liquid betainium bis(trifluoromethylsulfonyl)imide. *RSC Adv.* **2018**, *8*, 9299–9310. [[CrossRef](#)]
133. Abbott, A.P.; Capper, G.; Davies, D.L.; McKenzie, K.J.; Obi, S.U. Solubility of Metal Oxides in Deep Eutectic Solvents Based on Choline Chloride. *J. Chem. Eng. Data* **2006**, *51*, 1280–1282. [[CrossRef](#)]
134. Rodriguez Rodriguez, N.; Machiels, L.; Binnemans, K. *p*-Toluenesulfonic Acid-Based Deep-Eutectic Solvents for Solubilizing Metal Oxides. *ACS Sustain. Chem. Eng.* **2019**, *7*, 3940–3948. [[CrossRef](#)]
135. Abbott, A.P.; Capper, G.; Davies, D.L.; Rasheed, R.K.; Shikotra, P. Selective Extraction of Metals from Mixed Oxide Matrixes Using Choline-Based Ionic Liquids. *Inorg. Chem.* **2005**, *44*, 6497–6499. [[CrossRef](#)]
136. Tsuda, T.; Boyd, L.E.; Kuwabata, S.; Hussey, C.L. Electrochemistry of Copper(I) Oxide in the 66.7–33.3 mol % Urea–Choline Chloride Room-Temperature Eutectic Melt. *J. Electrochem. Soc.* **2010**, *157*, F96. [[CrossRef](#)]
137. Xie, X.; Zou, X.; Lu, X.; Xu, Q.; Lu, C.; Chen, C.; Zhou, Z. Electrodeposition behavior and characterization of copper–zinc alloy in deep eutectic solvent. *J. Appl. Electrochem.* **2017**, *47*, 679–689. [[CrossRef](#)]
138. Abbott, A.P.; Boothby, D.; Capper, G.; Davies, D.L.; Rasheed, R.K. Deep Eutectic Solvents Formed between Choline Chloride and Carboxylic Acids: Versatile Alternatives to Ionic Liquids. *J. Am. Chem. Soc.* **2004**, *126*, 9142–9147. [[CrossRef](#)]
139. Chen, W.; Jiang, J.; Lan, X.; Zhao, X.; Mou, H.; Mu, T. A strategy for the dissolution and separation of rare earth oxides by novel Brønsted acidic deep eutectic solvents. *Green Chem.* **2019**, *21*, 4748–4756. [[CrossRef](#)]
140. Shuwa, S.M.; Al-Hajri, R.S.; Jibril, B.Y.; Al-Waheibi, Y.M. Novel Deep Eutectic Solvent-Dissolved Molybdenum Oxide Catalyst for the Upgrading of Heavy Crude Oil. *Ind. Eng. Chem. Res.* **2015**, *54*, 3589–3601. [[CrossRef](#)]
141. Huang, P.; Zhang, Y. Electrodeposition of Nickel Coating in Choline Chloride-Urea Deep Eutectic Solvent. *Int. J. Electrochem. Sci.* **2018**, *13*, 10798–10808. [[CrossRef](#)]

142. Ru, J.; Hua, Y.; Xu, C.; Li, J.; Li, Y.; Wang, D.; Qi, C.; Jie, Y. Morphology-controlled preparation of lead powders by electrodeposition from different PbO-containing choline chloride-urea deep eutectic solvent. *Appl. Surf. Sci.* **2015**, *335*, 153–159. [[CrossRef](#)]
143. Ru, J.; Hua, Y.; Xu, C.; Li, J.; Li, Y.; Wang, D.; Qi, C.; Gong, K. Electrochemistry of Pb(II)/Pb during preparation of lead wires from PbO in choline chloride—Urea deep eutectic solvent. *Russ. J. Electrochem.* **2015**, *51*, 773–781. [[CrossRef](#)]
144. Yang, H.; Reddy, R.G. Fundamental Studies on Electrochemical Deposition of Lead from Lead Oxide in 2:1 Urea/Choline Chloride Ionic Liquids. *J. Electrochem. Soc.* **2014**, *161*, D586–D592. [[CrossRef](#)]
145. Billik, P.; Antal, P.; Gyepes, R. Product of dissolution of V₂O₅ in the choline chloride—urea deep eutectic solvent. *Inorg. Chem.* **2015**, *60*, 37–40.
146. Yang, H.; Reddy, R.G. Electrochemical Kinetics of Reduction of Zinc Oxide to Zinc Using 2:1 Urea/ChCl Ionic Liquid. *Electrochim. Acta* **2015**, *178*, 617–623. [[CrossRef](#)]
147. Yang, H.; Reddy, R.G. Electrochemical deposition of zinc from zinc oxide in 2:1 urea/choline chloride ionic liquid. *Electrochim. Acta* **2014**, *147*, 513–519. [[CrossRef](#)]
148. Liu, A.; Shi, Z.; Reddy, R.G. Electrodeposition of Zinc from Zinc Oxide in 2:1 Urea/1-Butyl-3-methylimidazolium Chloride Ionic Liquid. *J. Electrochem. Soc.* **2017**, *164*, D666–D673. [[CrossRef](#)]
149. Zheng, Y.; Dong, K.; Wang, Q.; Zhang, S.; Zhang, Q.; Lu, X. Electrodeposition of zinc coatings from the solutions of zinc oxide in imidazolium chloride/urea mixtures. *Sci. China Chem.* **2012**, *55*, 1587–1597. [[CrossRef](#)]
150. He, W.; Shen, L.; Shi, Z.; Gao, B.; Hu, X.; Xu, J.; Wang, Z. Zinc Electrodeposition from Zinc Oxide in the Urea/1-ethyl-3-methylimidazolium Chloride at 353 K. *Electrochemistry* **2016**, *84*, 872–877. [[CrossRef](#)]
151. Rimsza, J.M.; Corrales, L.R. Adsorption complexes of copper and copper oxide in the deep eutectic solvent 2:1 urea–choline chloride. *Comput. Theor. Chem.* **2012**, *987*, 57–61. [[CrossRef](#)]
152. Riaño, S.; Petranikova, M.; Onghena, B.; Vander Hoogerstraete, T.; Banerjee, D.; Foreman, M.R.S.; Ekberg, C.; Binnemans, K. Separation of rare earths and other valuable metals from deep-eutectic solvents: A new alternative for the recycling of used NdFeB magnets. *RSC Adv.* **2017**, *7*, 32100–32113. [[CrossRef](#)]
153. Tran, M.K.; Rodrigues, M.-T.F.; Kato, K.; Babu, G.; Ajayan, P.M. Deep eutectic solvents for cathode recycling of Li-ion batteries. *Nat. Energy* **2019**, *4*, 339–345. [[CrossRef](#)]



© 2019 by the authors. Licensee MDPI, Basel, Switzerland. This article is an open access article distributed under the terms and conditions of the Creative Commons Attribution (CC BY) license (<http://creativecommons.org/licenses/by/4.0/>).